by J. M. Ko, Y. Q. Ni and Q. L. Tian, Hong Kong Polytechnic

ABSTRACT

Empirical modeling of dynamic hysteretic behavior of a wire-cable vibration isolator is described. Experimental tests showed that, under steady periodic excitation, the dynamic hysteresis loops of the isolator depend on the vibration level, but are almost independent of vibration frequency. On these grounds, a simple mathematical model representing restoring force versus displacement, with amplitude-dependent parameters, is presented. This model is convenient for steady-state dynamic response analysis of nonlinear hysteretic systems. For identification of hysteresis loops of the isolator under steady harmonic motion, an alternative but direct procedure, based on the FFT and Chebyshev polynomial approach, is also proposed.

List of Symbols

A displacement amplitude

a displacement amplitude of harmonic motion

C factor of equivalent viscous damping

c coefficient

F restoring force

F_i, F'_i Fourier expansion coefficients of restoring force

$F_L(x)$ polynomial fitting to lower-side of hysteresis loop

F_{max} restoring force amplitude

$F_U(x)$ polynomial fitting to upper-side of hysteresis loop

F_1 "nonlinear nonhysteretic" force

F_2 "pure hysteretic" force

f frequency

$g(x), h(x)$ polynomial functions

K_e effective dynamic stiffness

k_1, k_2, k_3 coefficients

S_a hysteresis loop area

sgn sign function

$T_i(x/a)$ Chebyshev polynomial of the first kind

t time

$U_i(x/a)$ Chebyshev polynomial of the second kind

W_d energy dissipated by equivalent viscous damping force

$x, \dot{x}$ displacement and velocity

x_i, x'_i Fourier expansion coefficients of displacement

x' generalized velocity

Greek

α_i, β_i identified coefficients

Δ least square error

τ dimensionless time

ω circular frequency

Dr. J. M. Ko, Principal Lecturer, Department of Civil and Structural Engineering, Hong Kong Polytechnic, Kowloon, Hong Kong. Y. Q. Ni, Research Assistant, Hangzhou Architectural and Civil Engineering Institute, Hangzhou, China. Q. L. Tian, Research Fellow, the Institute of Mechanics, Chinese Academy of Sciences, Beijing, China.

Nonlinear vibration isolation is an effective and practical vibration control approach. Nonlinear vibration isolation techniques use nonlinear elastic and damping components (especially those with dry friction character) as the main vibration isolating devices. Compared with linear systems, nonlinear vibration isolation systems have the feature of both attenuating heavy shocks and absorbing wide-band vibrations.

The wire-cable vibration isolator, which is made by incorporating strands of closely-twisted stainless steel wire rope into two or more metal retainer bars, is a type of nonlinear vibration isolating device with friction damping characteristics. This isolator adopts stranded wire rope as the elastic component and utilizes inherent friction damping between individual rope strands.

Wire-cable isolator products are at present manufactured in the United States, Germany, China and other countries, and it is worthwhile to thoroughly investigate their dynamic characteristics and develop mathematical models for application. Only a few studies have been found so far [1-4]. For this kind of nonlinear isolator with dry friction damping properties, a significant proportion of its restoring force comes from internal rubbing, sliding and extruding. The restoring force-displacement curve of the isolator is thus macroscopically similar to the constitutive relation of elastoplastic material. Therefore, the restoring force depends not only on the instantaneous deformation, but also on the past history of deformation, possessing a hysteresis characteristic. The multi-valuedness of the restoring force corresponding to one value of displacement due to different past histories of deformation, makes it difficult to describe the dynamic performance of wire-cable isolators. With steady harmonic motion, a double-valued problem, for which two possible restoring forces exist for each displacement depending on the velocity sign, can be deduced.

This paper describes an experimental study of the dynamic hysteretic shear behavior of a wire-cable isolator under steady periodic excitations with a range of exciting frequencies and levels.

2. Dynamic Hysteretic Shear Tests

(a) Experimental Setup

The tested wire-cable vibration isolator is shown in Fig. 1. The steel wire ropes of the isolator are clustered in six bundles of 20 strands each, which are wrapped around a central wire cable. Several lengths
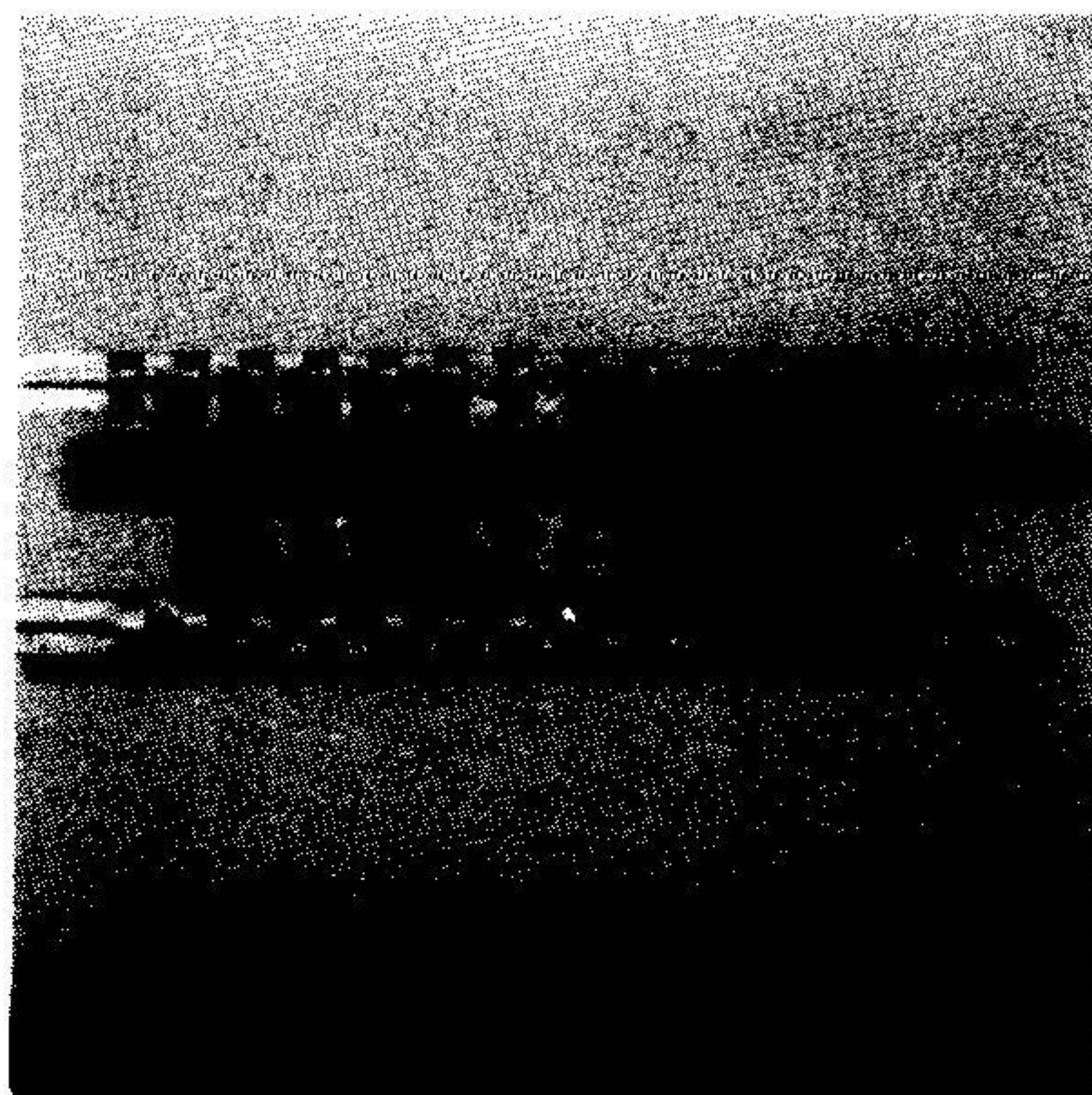

Fig. 1 Tested wire-cable vibration isolator

of the stranded wire rope are helically wound into a continuous series of 10 loops 2.5 cm in diameter, with each loop anchored at the top and bottom onto two aluminum retainer bars 10 cm in length.

Figure 2 illustrates the experimental setup for dynamic hysteretic behavior testing of the wire-cable isolator, arranged as a hanging shaking platform. This platform will be further used for vibration isolation tests of frame models incorporated with isolators. In this experimental setup, two rigid plates are hung in parallel on a trestle, through frictionless hinges connected with four rigid steel tubes, to form a double-pendulum system. Four guiding rollers, two on each side of the lower plate, prevent lateral movement of the system. The isolator is mounted and fixed with its aluminum retainer bars to the upper and lower plates for hysteretic shear behavior tests. The upper plate on top of the isolator is fixed horizontally to the trestle through a force transducer. The lower plate under the isolator is excited on one end and connected to an LVDT displacement transducer on the other. Since the deformation of the isolator is much smaller than the length of the hanging tubes, the relative movement between the two plates can cause an almost pure shear deformation in the isolator.

(b) Dynamic Behavior Tests

The excitation signal is supplied by a sine random generator via a power amplifier to the exciter, which harmonically drives the isolator. By varying the frequency and amplitude of the exciting signal, the corresponding restoring (hysteretic) force, acceleration and displacement signals are measured, synchronously recorded on a tape recorder, and observed with a digital signal analyzer. A total of 11
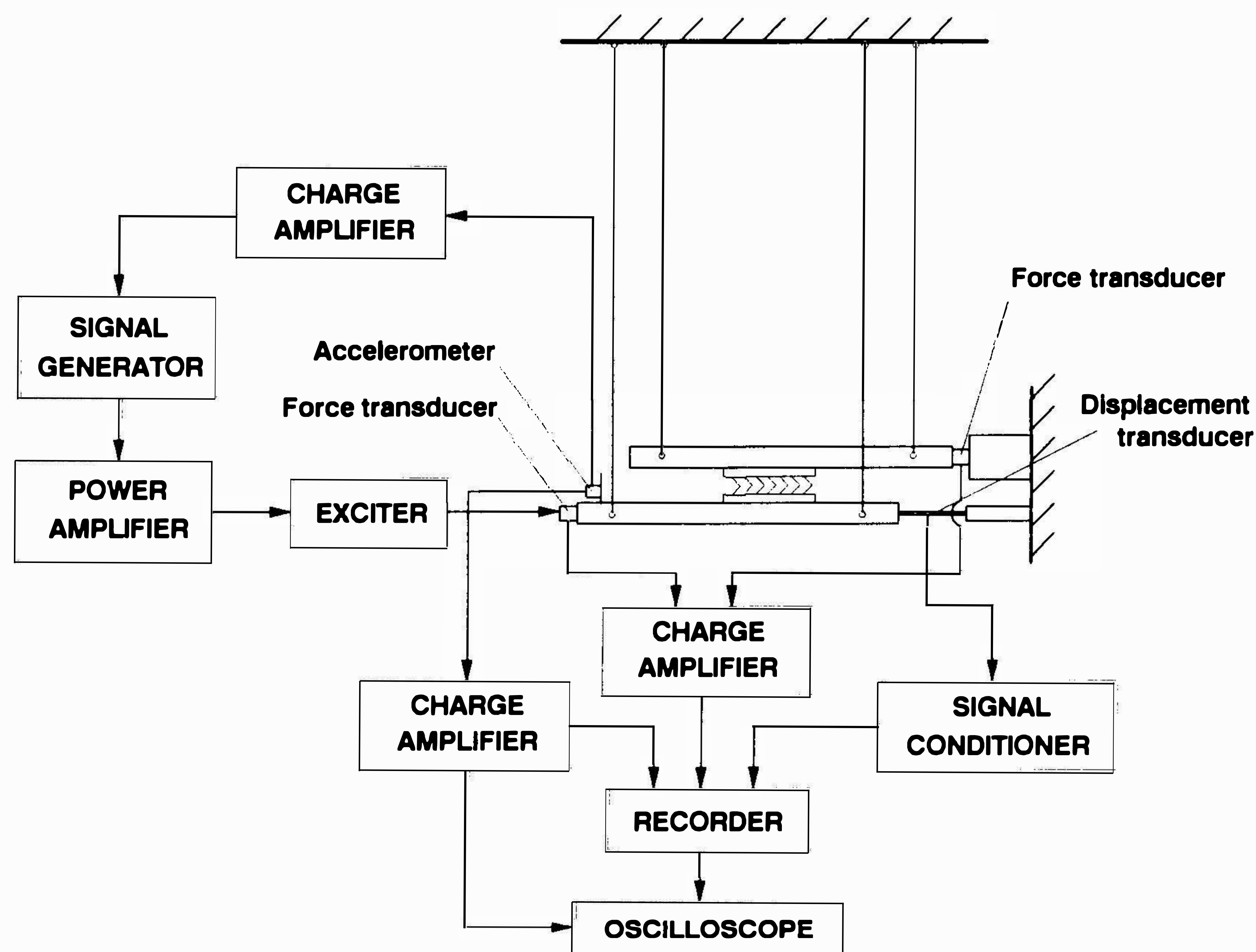

Fig. 2 A setup of hysteretic behavior testing

frequency values ranging from 5 Hz to 50 Hz, with at least 5 different amplitude levels in each case, were selected to test the dynamic hysteretic shear behavior of the isolator.

(c) Data Processing

The signals recorded on the tapes are reproduced and converted to digital data through an analog to digital I/0 board. They are further processed and analyzed by a program specially developed for hysteresis problems. The fast Fourier transform (FFT) is employed in the program for digital filtering and for calculating the Fourier expansion coefficients of these periodic digital signals. Calculating the Fourier coefficients of periodic signals by FFT is the main means for identifying hysteresis loops by Chebyshev polynomial expansion. If the digital acquisition of a periodic signal satisfies specified conditions, its Fourier expansion coefficients can be directly obtained by the FFT approach.

The following conditions must be satisfied for the FFT: the total number of digital data, K ($K=2^k$), used should be exactly M ($M=2^m$) integral cycles of the corresponding periodic signal; and each cycle also contains N ($N=2^n$) integral sampling points. That means $K = M \cdot N$ ($k = m+n$). Such $M \cdot N$ digital data can be sampled theoretically by taking the sampling rate equal to Nf where f is the frequency of the periodic signal. However, in practice the actual sampling rate in A/D conversion may be slightly different. Moreover, the frequency reading of the signal generator or signal analyzer may also be not exactly identical to the real frequency. The discrepancy of the sampling rate, though small, might result in distorted Fourier coefficients if the FFT is performed without any pre-processing of sampled data.

To eliminate the distortion, numerical re-sampling is processed before the FFT is performed in the program. According to the actual sampling rate in A/D conversion, the program recalculates the average frequency of M cycles of sampled data; then from this and by numerical interpolation, reforms K numerically-sampled data which conform to the preceding conditions. So long as the sampling rate in A/D conversion is large enough, the numerically re-sampled data still accurately reflect the original periodic signal. It is necessary for the sampled data used for the FFT to cover a great number of cycles, since the resolution frequency of the FFT is inversely proportional to the cycle number, and the averaging of many cycles is conducive to improving precision and reducing noise influence.

TABLE 1   THE FOURIER EXPANSION COEFFICIENTS OF RECORDED SIGNALS

	Harmonic No.		1st	2nd	3rd	4th	5th	6th
6 Hz	x (mm)	x_i	1.8569	-0.0180	0.0186	-0.0010	0.0016	-0.0002
		x_i'	-0.0266	0.0241	-0.0078	0.0008	0.0005	0.0000
	F (N)	F_i	17.2279	-0.3872	2.9931	-0.1804	1.0298	-0.1231
		F_i'	-10.21	0.7799	-0.3816	0.1922	0.3820	0.0563
25 Hz	x (mm)	x_i	0.2360	0.0002	0.0001	0.0000	0.0000	0.0000
		x_i'	0.0006	0.0000	0.0000	0.0000	0.0000	0.0000
	F (N)	F_i	8.0243	-0.0773	0.6690	-0.0122	0.0280	0.0097
		F_i'	-2.5274	0.0153	0.5002	-0.0143	0.1098	-0.0041

Nonsynchronism of the restoring force and displacement signals during recording and sampling will seriously distort the shape and area of the hysteresis loop. Therefore, these two signals should be simultaneously measured at each recording instant, and then sampled with synchronous and high speed data acquisition processors. On the other hand, the displacement output of the charge amplifier by integrating input accelerometer signals with its built-in integrator, generally possesses certain phase shift error, especially for high frequency signals. Therefore in the case of high frequency, the displacement data needed for hysteresis analysis should be obtained by the numerical integration of recorded acceleration signals [5].

Table 1 shows the Fourier expansion coefficients of the isolator displacement and restoring force periodic signals recorded for exciting frequencies at 6 and 25 Hz. Here x_i and F_i are associated with cosine terms while x_i' and F_i' are associated with sine terms. It can be seen that the isolator is not in purely simple harmonic motion, particularly in the case of low frequency and large excitation. All the Fourier coefficient values corresponding to each exciting frequency and level have been calculated and will be used in identifying hysteresis loops by the Chebyshev polynomial approach.

(d) Hysteresis Loops

Four varieties of hysteresis loops corresponding to one group of displacement and restoring force signals are illustrated in Figs. 3(a-d). Fig. 3(a) shows the loops without filtering, 3(b) shows the loops after filtering, 3(c) shows the loops obtained by inverse FFT only to the Fourier coefficients of harmonic terms, and 3(d) is the power polynomial fit to the loops shown in 3(b). In Fig. 3(c) two loops are presented, the dotted-line one includes all harmonics, and the solid-line one, for which only odd harmonics were chosen, is symmetric about the origin. Physically, the shear restoring force of a wire-cable isolator is antisymmetric with respect to its displacement under harmonic motion. Therefore, in Fig. 3(d), two mutually-odd power polynomial functions, representing the upper-side and lower-side of the loop, were selected to fit the experimental data.
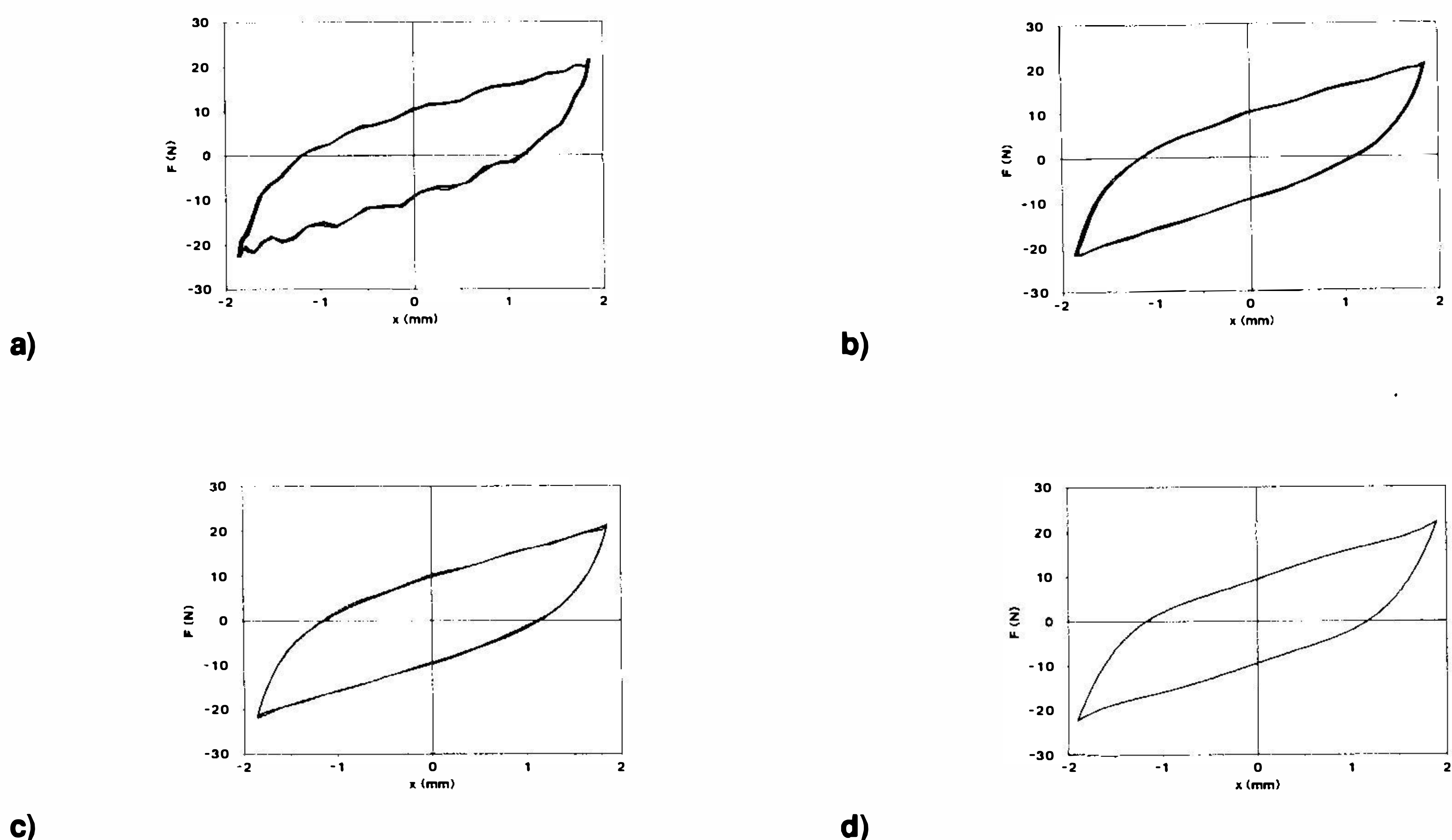
a)

b)

c)

d)

Fig. 3 Hysteresis loops of the isolator

The fitted polynomial functions of hysteresis loops will be further used for establishing a mathematical model of the isolator. The coefficients of these functions are obtained by the least square fit to experimental loops after filtering. Suppose the upper-side of the fitted hysteresis loop is a fifth order power polynomial function, i.e.,

$$\begin{aligned} F_U(x) &= a_0 + a_1 x + a_2 x^2 + a_3 x^3 + a_4 x^4 + a_5 x^5 \\ &= a_1 x + a_3 x^3 + a_5 x^5 + \left(a_0 + a_2 x^2 + a_4 x^4\right) \quad \text{for } \dot{x} > 0 \end{aligned} \tag{1}$$

According to the antisymmetry the lower side should be

$$\begin{aligned} F_L(x) &= -a_0 + a_1 x - a_2 x^2 + a_3 x^3 - a_4 x^4 + a_5 x^5 \\ &= a_1 x + a_3 x^3 + a_5 x^5 - \left(a_0 + a_2 x^2 + a_4 x^4\right) \quad \text{for } \dot{x} < 0 \end{aligned} \tag{2}$$

Eqs. (1) and (2) can be written in unified form

$$\begin{aligned} F(x, \dot{x}) &= a_1 x + a_3 x^3 + a_5 x^5 + \left(a_0 + a_2 x^2 + a_4 x^4\right) \cdot sgn(\dot{x}) \\ &= g(x) + h(x) \cdot sgn(\dot{x}) \end{aligned} \tag{3}$$
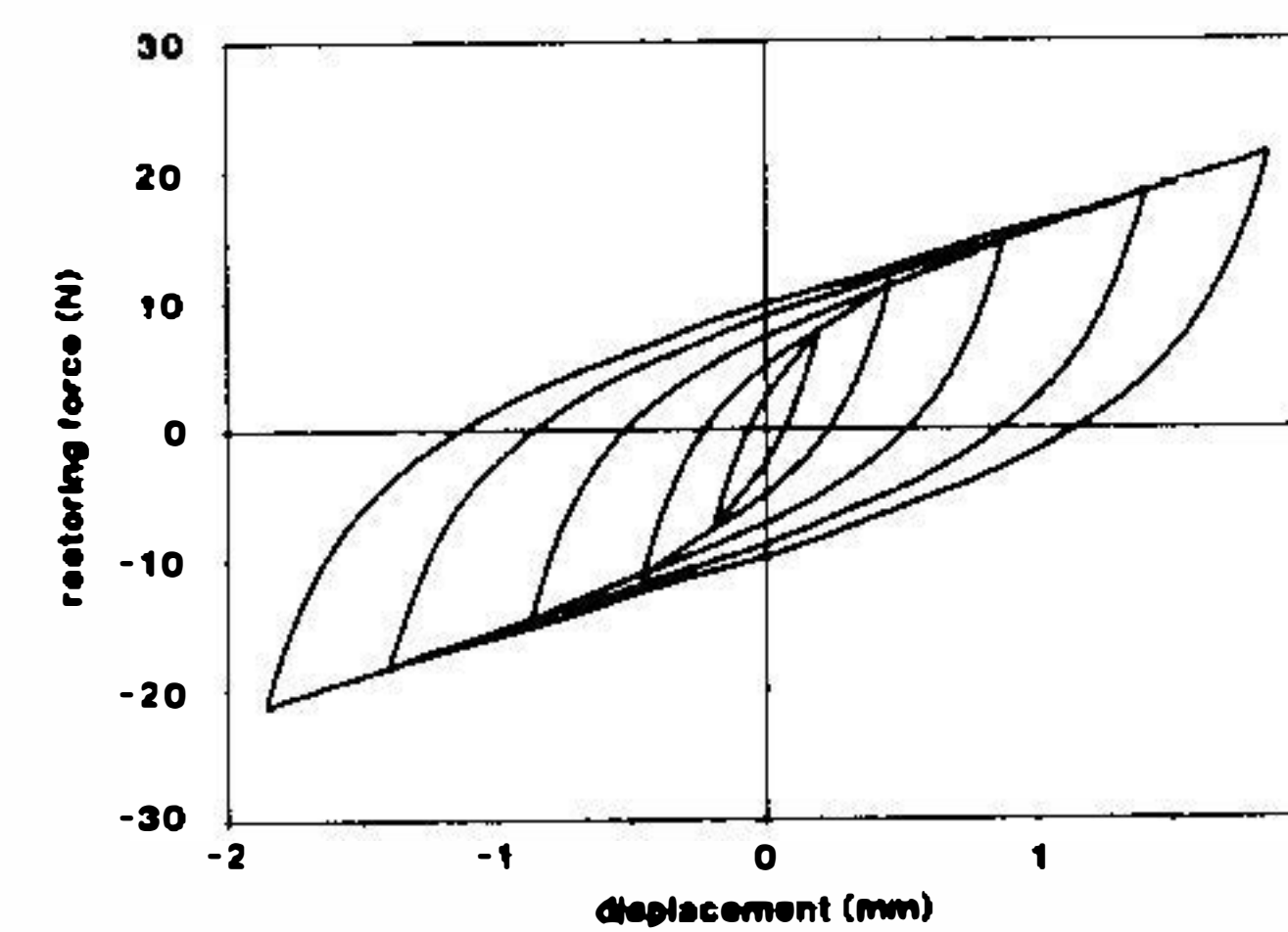
in which

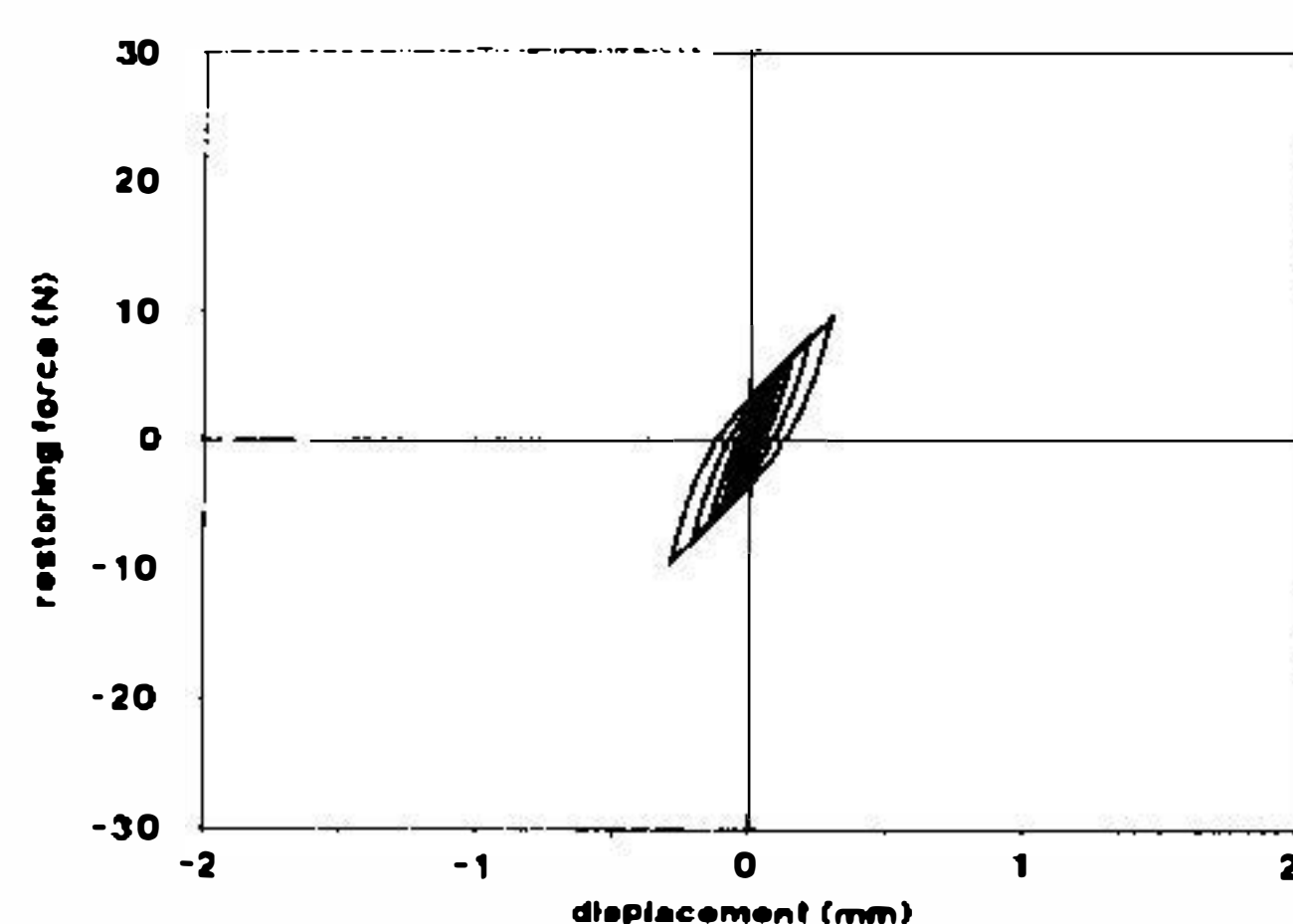$$g(x) = a_1 x + a_3 x^3 + a_5 x^5$$

$$h(x) = a_0 + a_2 x^2 + a_4 x^4$$

Let (x_n, y_n) for $n = 1, 2, \cdots, N$ be all upper-side discrete points of the filtered experimental hysteresis loops corresponding to a certain group of displacement and restoring force signals, and (x_m, y_m) for
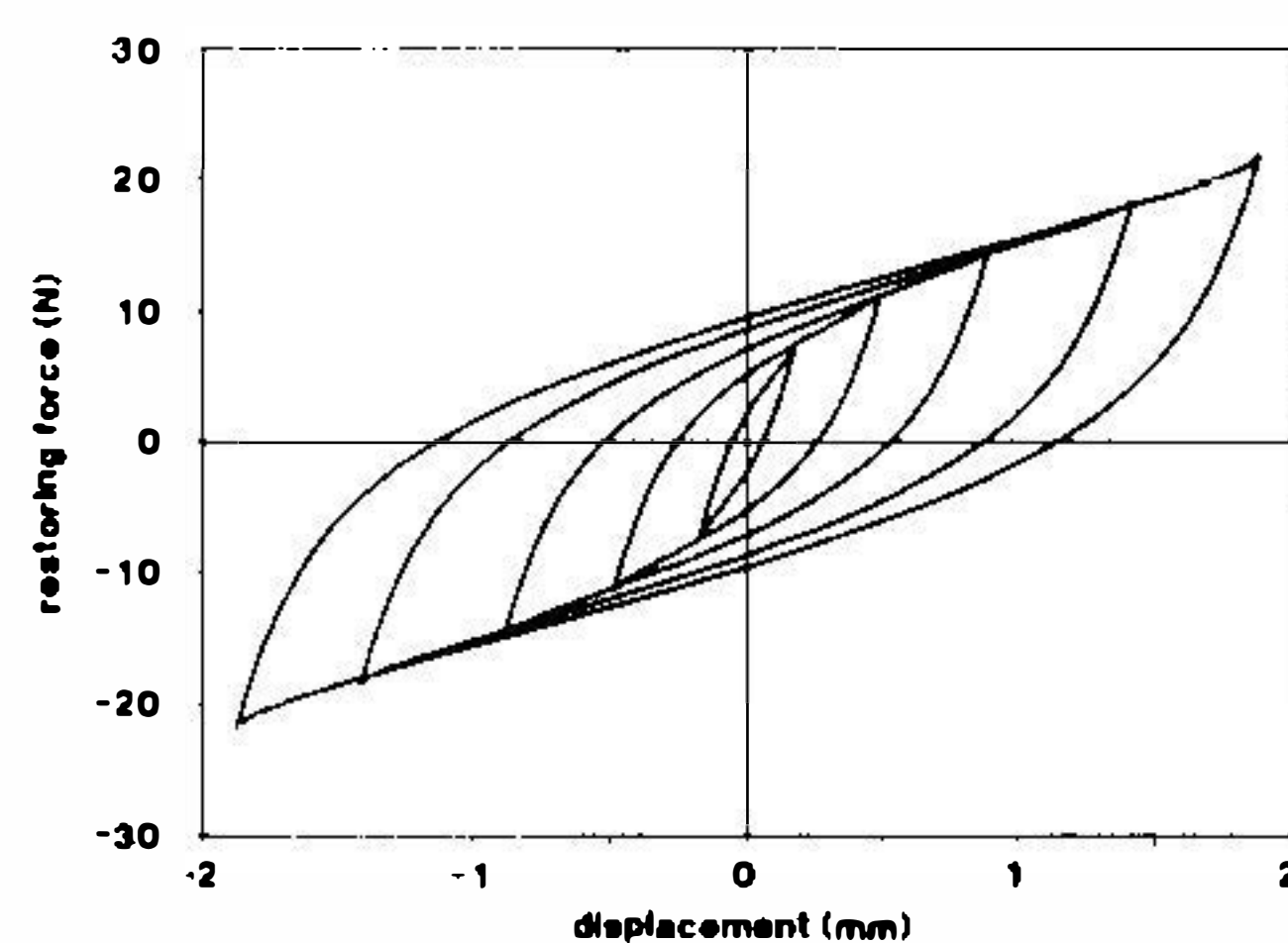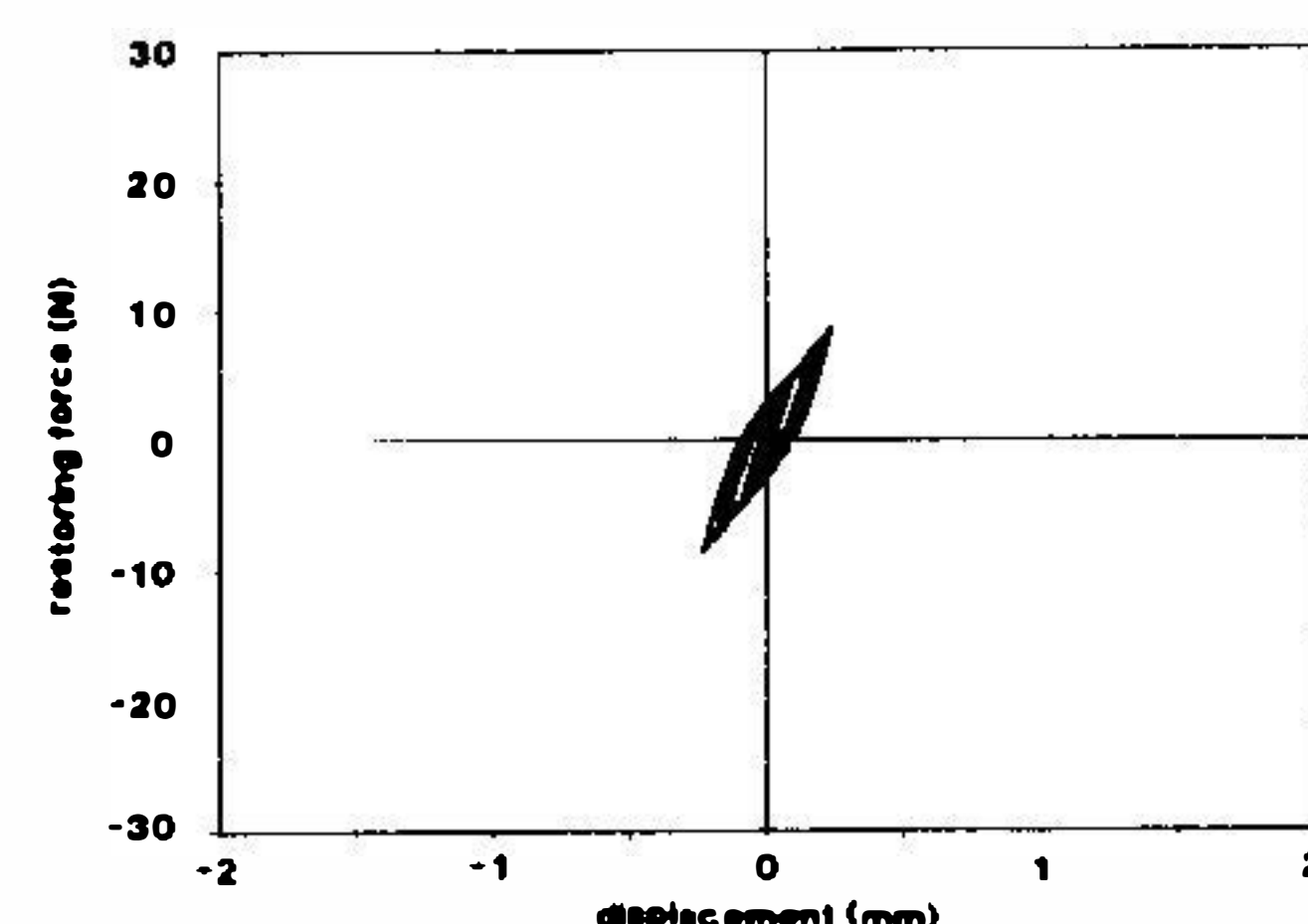

a)

b)

c)

d)

Fig. 4 Hysteresis loops: restoring force against displacement

m = 1,2,···, M be all lower-side discrete points. If the Kth order power polynomial functions are selected to fit the loops, then

$$F_U(x) = \sum_{j=0}^{K} a_j x^j \qquad \text{for } \dot{x} > 0 \qquad (4)$$

$$F_L(x) = \sum_{j=0}^{K} (-1)^{j+1} a_j x^j \qquad \text{for } \dot{x} < 0 \qquad (5)$$

and applying the least square method,in which the least square error is

$$\Delta = \sum_{n=1}^{N} \left[y_n - F_U(x_n) \right]^2 + \sum_{m=1}^{M} \left[y_m - F_L(x_m) \right]^2 \qquad (6)$$

Let $\dfrac{\partial \Delta}{\partial a_j} = 0$ $(j = 0,1,2,···, K)$, then solve a $(K+1)$th order system of linear algebraic equations to get the values of a_j $(j = 0,1,2,···, K)$. For each group of experimental hysteresis loops corresponding to a certain frequency and displacement amplitude, we can obtain corresponding values of fitted coefficients a_j $(j = 0,1,2,···, K)$. Therefore, conceptually these coefficients are functions of frequency ω and amplitude A.

Figures 4 and 5 are the hysteresis loops at 6, 9, 20 and 25 Hz with different amplitudes obtained by the FFT approach. Figure 4 shows the isolator restoring force against displacement. Figure 5 shows the isolator restoring force against velocity. It can be seen that the restoring force of the wire-cable isolator exhibits typical hysteretic nonlinearity.
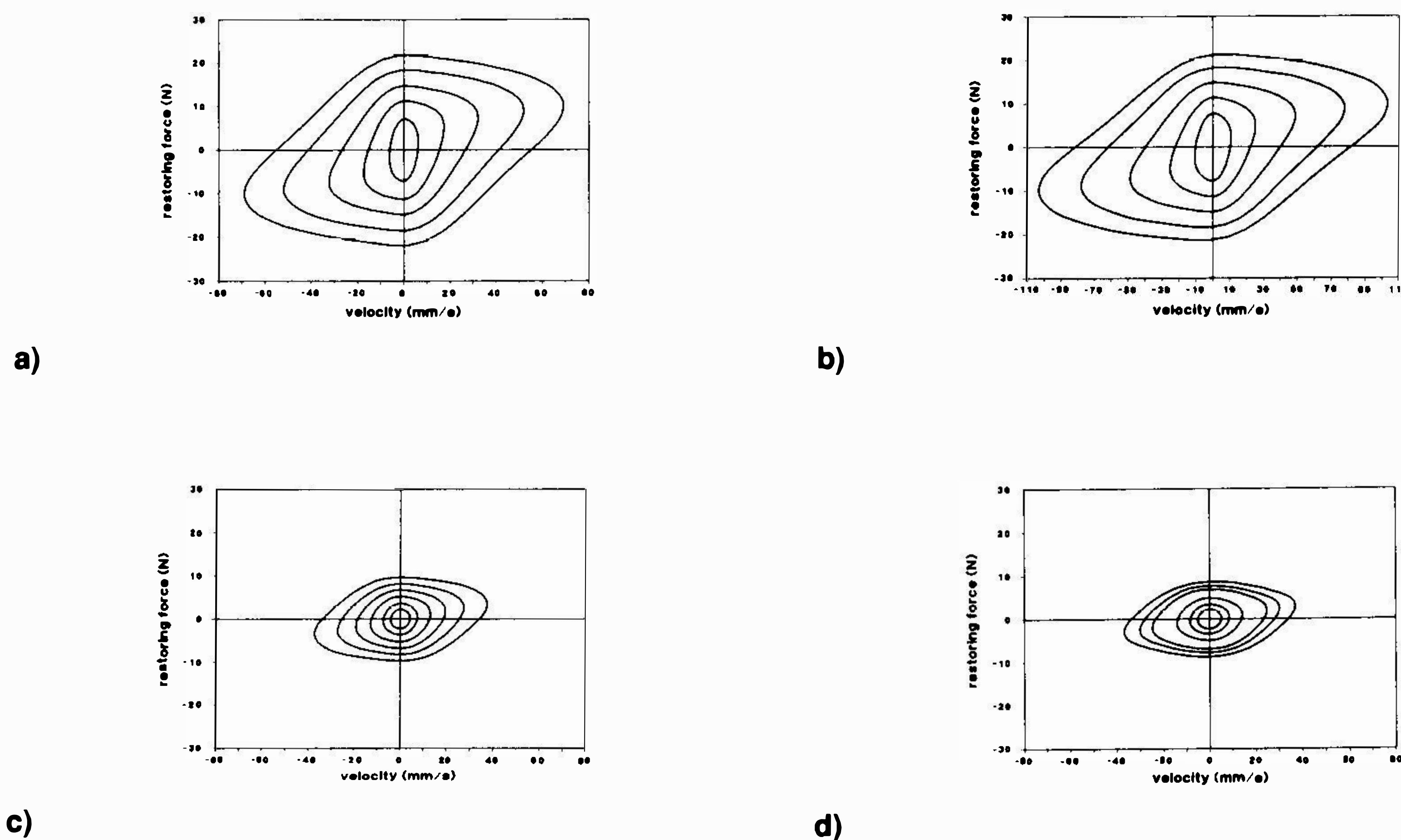

a)

b)

c)

d)

Fig. 5 Hysteresis loops: restoring force against velocity

Comparing all hysteresis loops of the same scale ranging from 5 to 50 Hz with different amplitudes, it can be seen that the hysteresis loops of restoring force versus displacement depend only on amplitude A and are independent of frequency ω. This conclusion is in accord with the physical constitutive relation, and will make the description of hysteretic behavior convenient.

(e) Effective Stiffness and Area of Hysteresis Loop

The effective dynamic shear stiffness (geometric stiffness) values of the wire-cable isolator under various frequencies and amplitudes are illustrated in Fig. 6. The effective stiffness is defined as

$$K_e = \frac{F_{max} - F_{min}}{X_{max} - X_{min}} \tag{7}$$

It is also shown in Fig. 6 that the effective stiffness, K_e, varies only with amplitude, A, and frequency, ω, has no influence on it. This is consistent with the conclusion above. The effective stiffness, K_e, monotonically decreases as amplitude A increases. This indicates that the wire-cable isolator possesses softening dynamic shear stiffness. In Fig. 6, the continuous curve is of the fitted function of K_e versus A. This function is expressed as

$$K_e = K_e(A) = -4.725 + 21.343 \cdot A^{-0.409} \tag{8}$$

Similarly, the hysteresis loop area, S_a, being the energy dissipated per cycle, is also only a function of amplitude A as shown in Fig. 7. S_a increases progressively as amplitude A increases. It is approximately
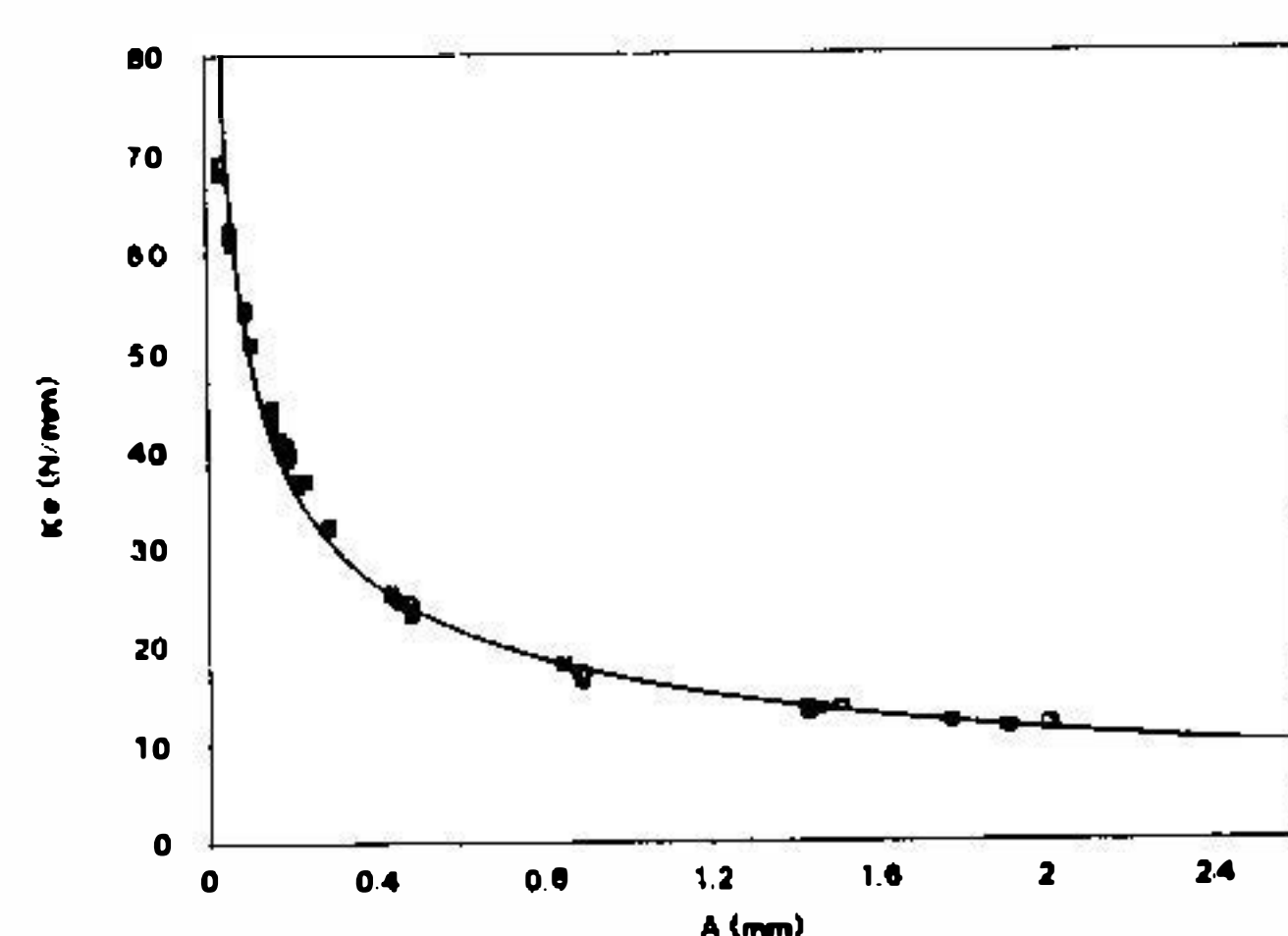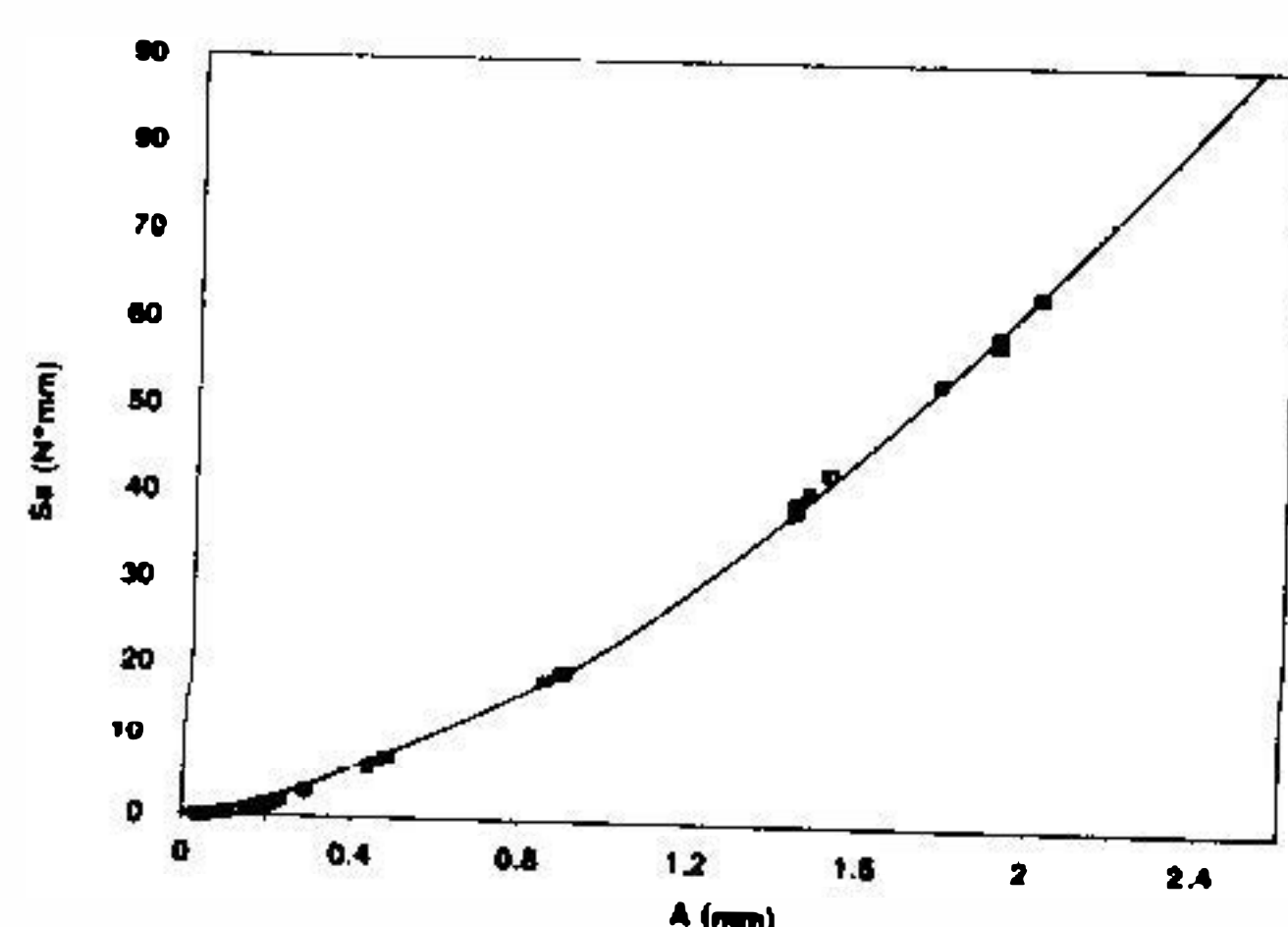

Fig. 6 Effective dynamic stiffness
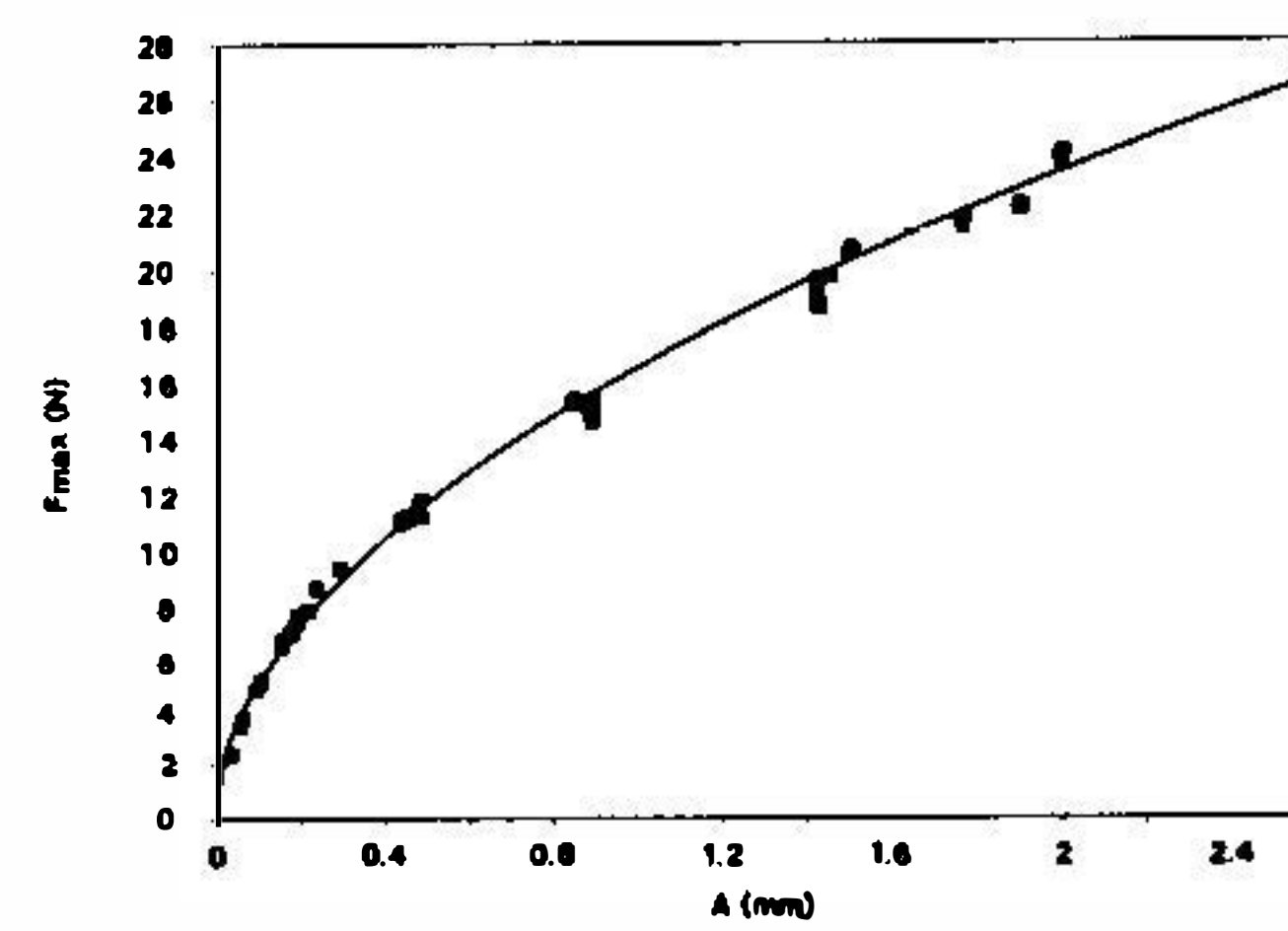

Fig. 7 Hysteresis loop area

Fig. 8 Restoring force amplitude

directly proportional to amplitude A when A is large, which reflects the expansion fashion of the hysteresis loop of the wire-cable isolator with amplitude. A simple power function is used to fit the curve of S_a against A, i.e.,

$$S_a = S_a(A) = 22.578 \cdot A^{1.494} \tag{9}$$

Restoring force amplitude, F_{max}, varies only with displacement amplitude A as shown in Fig. 8. The relationship of F_{max} versus A also reflects the softening stiffness characteristic of wire-cable isolators. It is noted that F_{max} exhibits an approximately linear increasing relation to A when A is large. This is similar to the S_a-A curve with large A. These two nearly directly proportional relations are helpful for comprehending the hysteresis loop feature in large amplitude cases. In Fig. 8, the continuous curve shows the fitted function as

$$F_{max} = F_{max}(A) = 16.568 \cdot A^{0.497} \tag{10}$$

3. A Mathematical Model with Amplitude-Dependent Parameters

In order to analyze the dynamic response of vibration isolated systems with wire-cable isolators, a mathematical model of this isolator should be built. For the hysteretic isolator, due to the multi-valuedness of restoring force about displacement, it is difficult to present a mathematical model which really reflects the hysteretic characteristic of the isolator. The relationship between restoring force F and displacement x is not an explicit function and not holonomic. It depends, as well, on the sign of the velocity $\dot{x}$ and on the previous history of the motion. A differential mode, the Bouc-Wen model proposed initially by Bouc [6] and further extended by Wen [7], is usually applied to describe hysteretic systems. Although this differential model has been widely used in the random response analysis of hysteretic dynamic systems
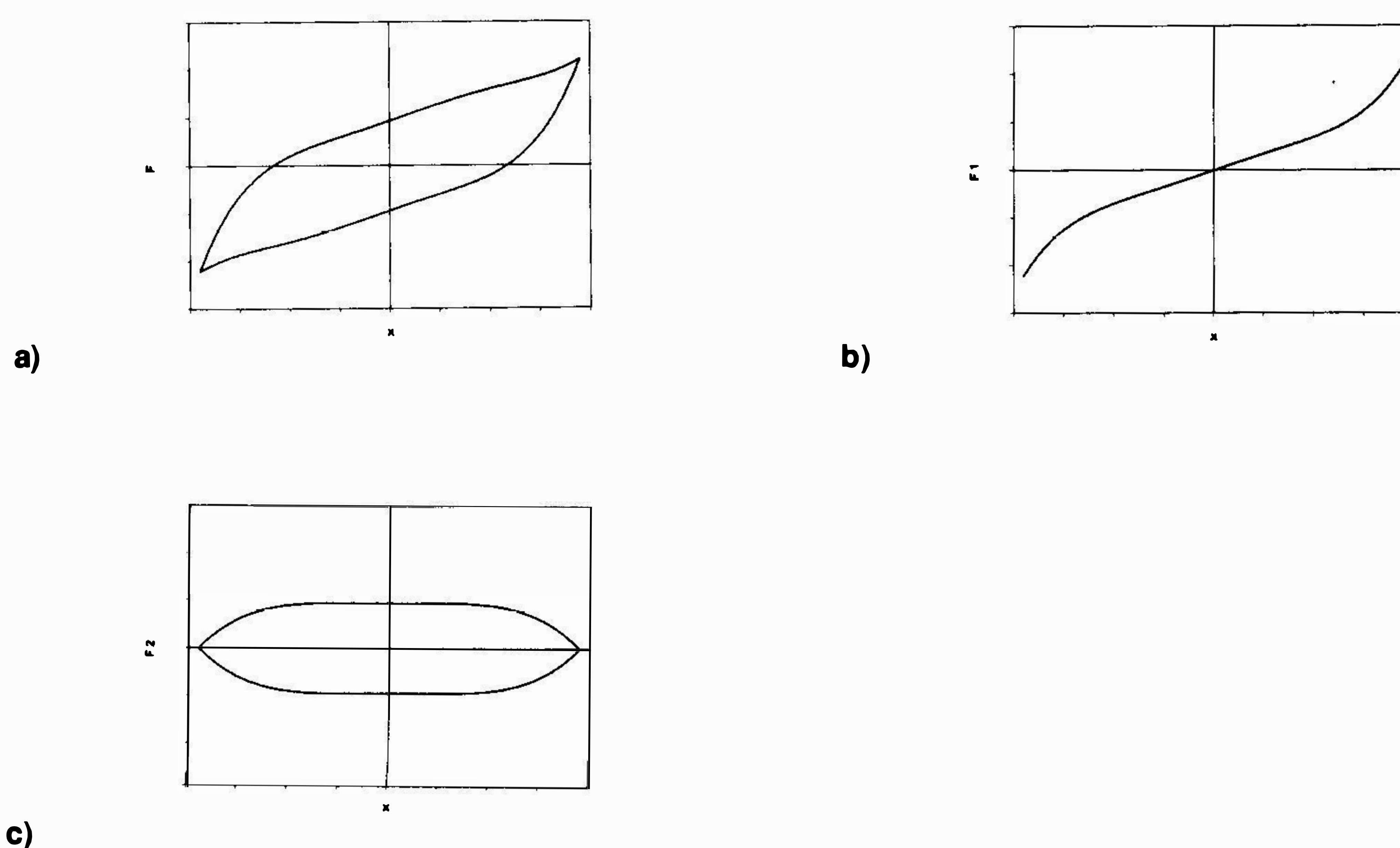
a)

b)

c)

Fig. 9 Restoring force and its decomposition

[8-10], it is difficult and inconvenient to compute the steady-state dynamic responses of hysteretic systems by adopting this model.

Some alternative procedures based on averaging and equivalence can be applied to establish rational mathematical models for hysteretic systems, e.g., the trace method [11,12]. In this section, a simple mathematical model of the isolator, with amplitude-dependent parameters, is presented based on the same approach.

The restoring force of a hysteretic isolator may be decomposed into two parts, "nonlinear nonhysteretic" force and "pure hysteretic' force. The former is expressed by a single-valued nonlinear function in the displacement-force plane, related to the hysteresis loop shape and with amplitude-dependent coefficients. The latter, which is approximated by an ellipse with the same amplitude and the same area as the corresponding hysteresis loop, is substituted with an equivalent viscous damping function having amplitude- and frequency-dependent coefficients.

From Eqs. (1) to (3), the averaging curve of the upper side and the lower side of the hysteresis loop under steady periodic motion can be written as

$$F_a(x) = [F_U(x) + F_L(x)]/2$$
$$= a_1 x + a_3 x^3 + a_5 x^5 = g(x) \tag{11}$$

Thus, the hysteresis loop of Fig. 9(a) may be split into $g(x)$ of Fig. 9(b) and $h(x) \cdot sgn(\dot{x})$ of Fig. 9(c). Therefore, the "nonlinear nonhysteretic" force function of the wire-cable isolator may be expressed as

$$F_1 = F_1(x, A) = k_1(A) \cdot x + k_2(A) \cdot x^3 + k_3(A) \cdot x^5 \tag{12}$$

If the "pure hysteretic" loop defined by $h(x) \cdot sgn(\dot{x})$ is replaced with an equivalent viscous damping, the "pure hysteretic" force function of the isolator may be expressed as
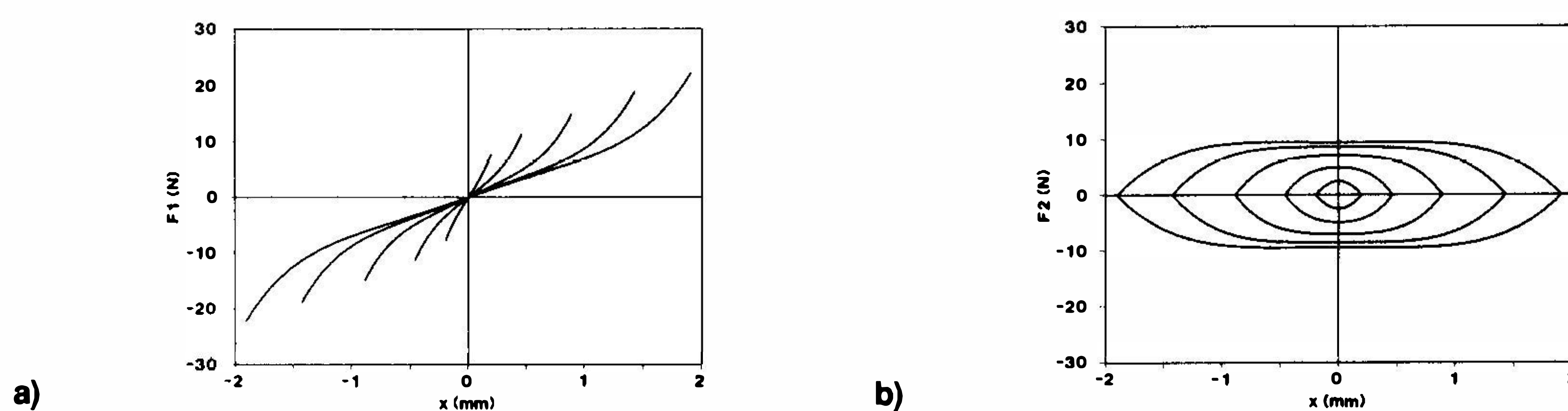
a)

b)

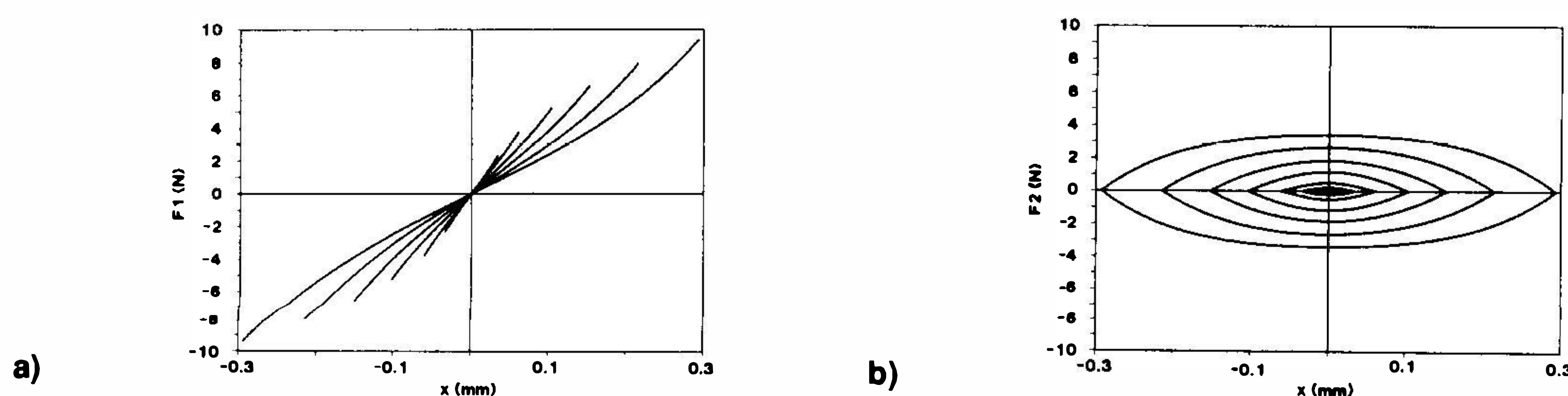**Fig. 10 Decomposition of hysteresis loops at 9 Hz**

a)

b)

Fig. 11 Decomposition of hysteresis loops at 20 Hz

$$F_2 = F_2(\dot{x}, A) = C(A, \omega) \cdot \dot{x} \tag{13}$$

The mathematical model of the wire-cable isolator, i.e., the restoring force-displacement relation, is then given as

$$F(x, \dot{x}, A) = F_1(x, A) + F_2(\dot{x}, A)$$
$$= k_1(A) \cdot x + k_2(A) \cdot x^3 + k_3(A) \cdot x^5 + C(A, \omega) \cdot \dot{x} \tag{14}$$

The expressions for the coefficients $k_1(A)$, $k_2(A)$, $k_3(A)$ and $C(A, \omega)$ are determined as follows. The "nonlinear nonhysteretic" forces and the "pure hysteretic" forces separated from the hysteresis loops at 9 and 20 Hz, are shown in Figs. 10 and 11 for a range of amplitudes. It can be seen that the expressions for $k_1(A)$, $k_2(A)$, $k_3(A)$ can be obtained by fitting all the "nonlinear nonhysteretic" force-displacement curves with different amplitudes and frequencies, and theoretically, can be directly determined by fitting the values of a_1, a_3 and a_5 respectively.

The function $k_1(A)$ physically means the initial stiffness of the isolator against amplitude A, i.e.,

$$k_1(A) = \left. \frac{\partial F_1(x, A)}{\partial x} \right|_{x=0} \tag{15}$$

It is directly worked out by fitting all the values of the average initial stiffness, i.e., all the a_1 values for different amplitudes and frequencies. The fitted function of $k_1(A)$ is expressed as

$$k_1(A) = -1.760 + 12.408 \cdot A^{-0.539} \tag{16}$$

The initial stiffness values corresponding to different amplitudes and frequencies as well as the fitted $k_1(A)$ are illustrated in Fig. 12.

The functions $k_2(A)$ and $k_3(A)$ can be theoretically obtained by directly fitting the known a_3 and a_5 values, respectively. However, the values of a_3 and a_5 themselves are coefficients of higher order terms acquired by fitting hysteresis loops, and scattered. Good fitting for $k_2(A)$ and $k_3(A)$ is not likely. It is suggested in the present paper that the expressions of $k_2(A)$ and $k_3(A)$ could be defined after determining both the values of $F_1(x, A)$ and its derivative at $x = A$.

When $x=A$, $F_1(x, A)$ should be equal to $F_{max}(A)$, i.e.,

$$F_1(x, A)\big|_{x=A} = k_1(A) \cdot A + k_2(A) \cdot A^3 + k_3(A) \cdot A^5 = F_{max}(A) \tag{17}$$
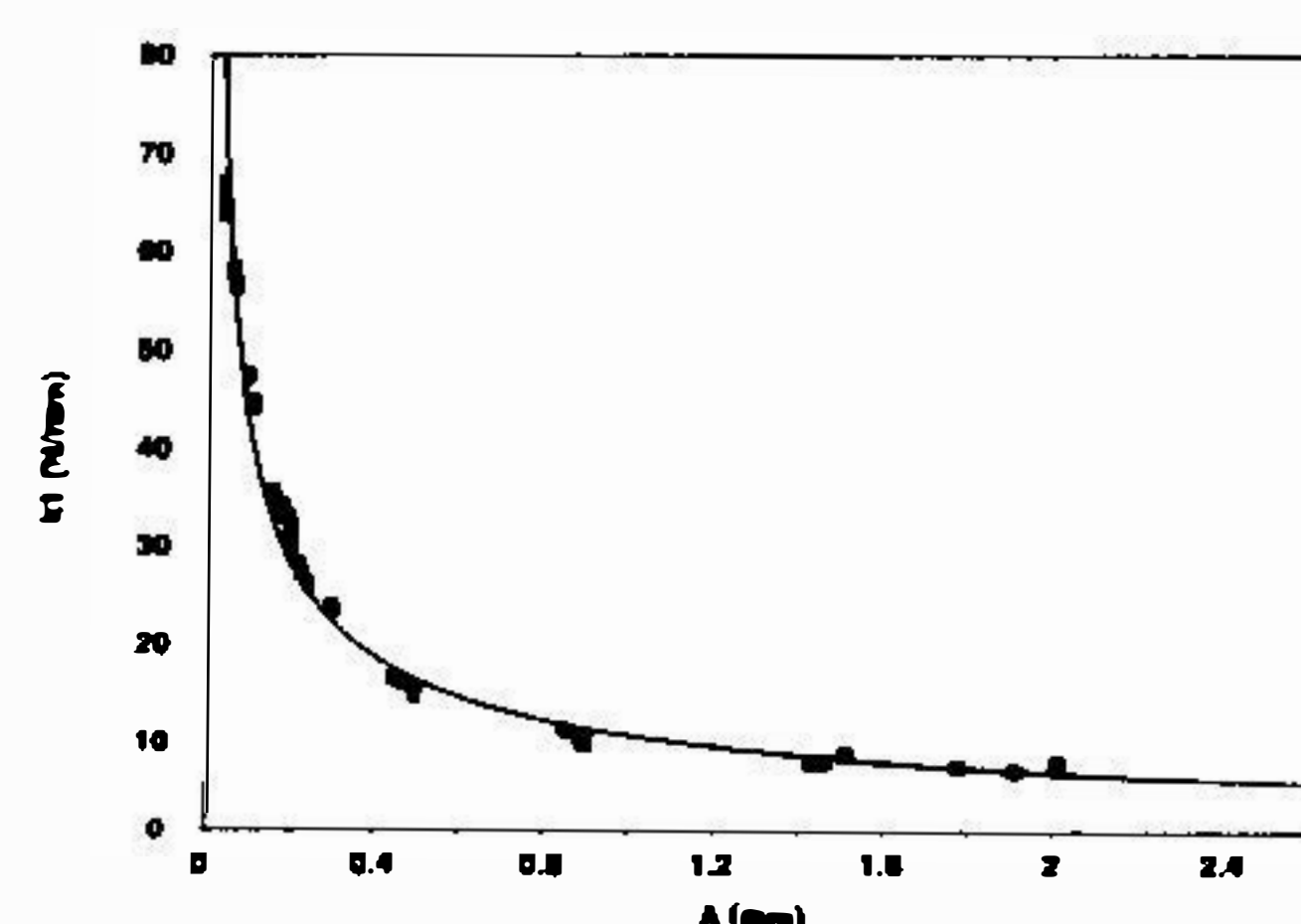
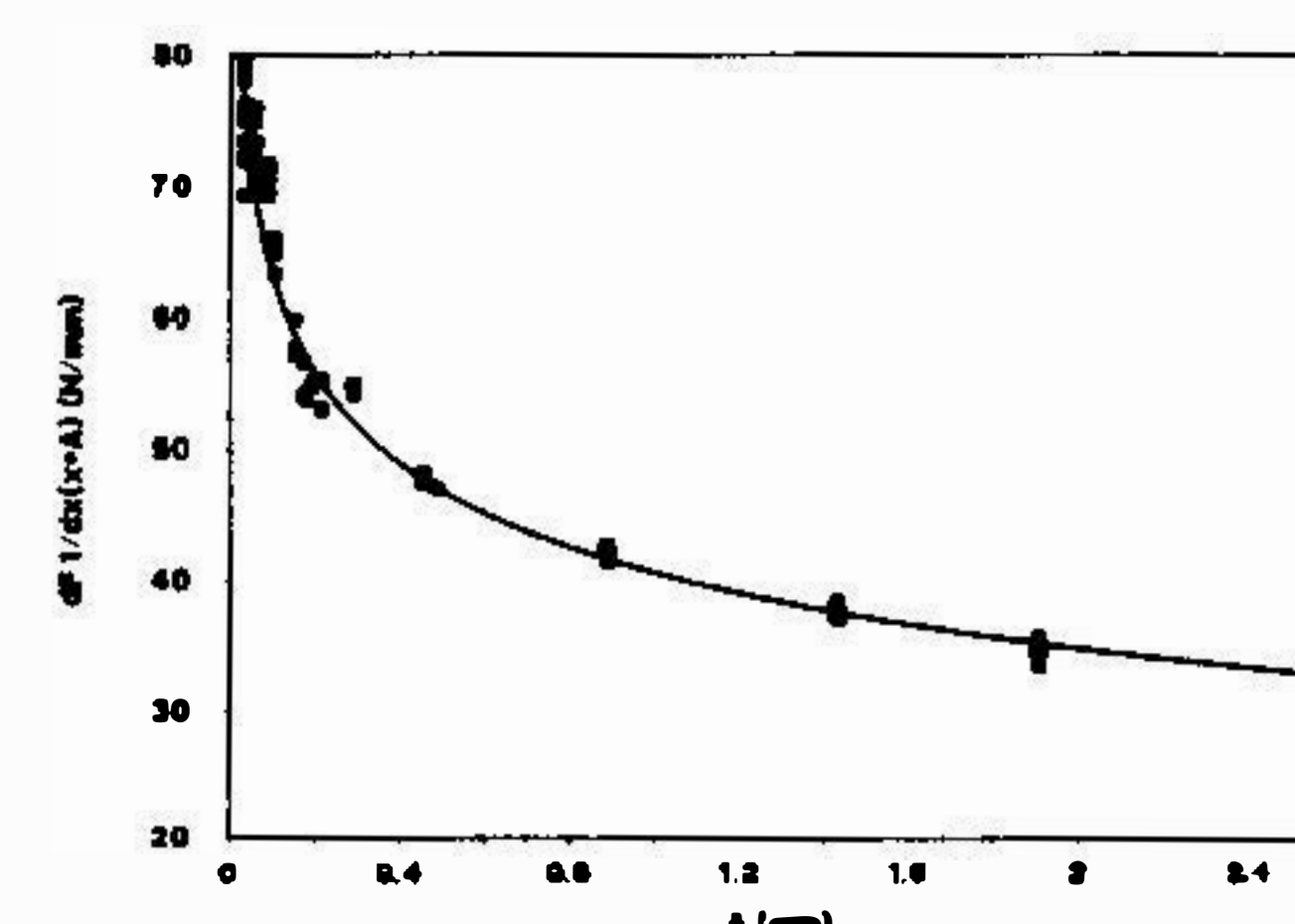**Fig. 12 Coefficient function $k_1(A)$**   **Fig. 13 The average slope at $x = A$**

Substituting Eqs. (10) and (16) into Eq. (17), yields

$$-1.760 \cdot A + k_2(A) \cdot A^3 + k_3(A) \cdot A^5 = 16.568 \cdot A^{0.497} - 12.408 \cdot A^{0.461} \tag{18}$$

The average slope of the upper and lower sides of hysteresis loops at $x = A$, is defined as

$$\left. \frac{dF_1}{dx} \right|_{x=A} = \frac{1}{2} \left[\left. \frac{dF_U(x)}{dx} \right|_{x=A} + \left. \frac{dF_L(x)}{dx} \right|_{x=A} \right] \tag{19}$$

The values of the average slope at $x = A$ and corresponding fitted function are shown in Fig. 13. The expression of the fitted function is

$$\left. \frac{dF_1}{dx} \right|_{x=A} = -38.695 + 79.223 \cdot A^{-0.109} \tag{20}$$

Substituting Eqs. (12) and (16) into Eq. (20), yields

$$36.935 + 3 \cdot k_2(A) \cdot A^2 + 5 \cdot k_3(A) \cdot A^4 = 79.233 \cdot A^{-0.109} - 12.408 \cdot A^{-0.539} \tag{21}$$

According to Eqs. (18) and (21), the expressions of $k_2(A)$ and $k_3(A)$ are derived, namely,

$$k_2(A) = +22.867 \cdot A^{-2} - 39.612 \cdot A^{-2.109} + 41.420 \cdot A^{-2.503} - 24.816 \cdot A^{-2.539} \tag{22}$$

$$k_3(A) = -21.107 \cdot A^{-4} + 39.612 \cdot A^{-4.109} - 24.852 \cdot A^{-4.503} + 12.408 \cdot A^{-4.539} \tag{23}$$

Substituting the expressions of $k_1(A)$, $k_2(A)$, $k_3(A)$ into Eq. (12) gives the expression of $F_1(x,A)$. For the sake of checking the accuracy of $F_1(x,A)$ thus obtained, the function curves of $F_1(x,A)$ by virtue of Eq. (12) are shown in Figs. 14(a-b), respectively with the same amplitudes as those obtained experimentally at 9 and 20 Hz. It can be seen by comparing Figs. 10(a) and 11(a), the function $F_1(x,A)$ given above properly expresses the "nonlinear nonhysteretic" force of the isolator.

The expression $F_2(\dot{x},A)$ of the equivalent viscous damping force, approximating the "pure hysteretic" force, is derived by virtue of energy equivalence. The energy dissipated per cycle of the isolator, i.e., the hysteresis loop area $S_a(A)$, has been obtained by Eq. (9). Correspondingly, the energy dissipated by the equivalent viscous damping force per cycle, W_d, under cyclic motion with the same amplitude, is

$$W_d = \int_{-A}^{A} C(A, \omega) \cdot \dot{x} dx = \pi \cdot C(A, \omega) \cdot A^2 \cdot \omega \tag{24}$$

For equivalent energy dissipation, let $S_a = W_d$, to get

$$C(A, \omega) = S_a(A) / \left(\pi \cdot \omega \cdot A^2 \right) = 7.187 \cdot A^{-0.506} / \omega \tag{25}$$

In steady-state periodic response analysis, the dimensionless time, $\tau = \omega t$, is generally introduced, and the generalized velocity is defined as

$$x' = \frac{dx}{d\tau} = \omega^{-1} \frac{dx}{dt} = \frac{\dot{x}}{\omega} \qquad (26)$$

so another expression of function $F_2(\dot{x},A)$ can be obtained as follows

$$F_2(x',A) = c(A) \cdot x' \qquad (27)$$

in which

$$c(A) = 7.187 \cdot A^{-0.506} \qquad (28)$$

The function curves of $F_2(\dot{x},A)$ thus obtained, respectively, with the same amplitudes as those obtained experimentally at 9 and 20 Hz, are illustrated in Figs. 15(a-b). The equivalence can be clarified by comparison with Figs. 10(b) and 11(b).

So far the mathematical model of the wire-cable isolator, i.e., the relationship of restoring force versus displacement, has been presented. A corresponding multi-harmonic steady state response computational method for the analysis of vibration-isolated structures, with nonlinear hysteretic isolators adopting the amplitude-dependent model above, has been also presented [13].

4. A Simple Approach to Identify Hysteresis Loops

In the dynamic hysteretic behavior experiment of the wire-cable isolator mentioned above, the isolator is excited to achieve steady harmonic motion. When the isolator under test exhibits simple harmonic motion, based on the determined Fourier coefficients of recorded signals and by applying the Chebyshev polynomial approach [14], the function expressions of hysteresis loops can be identified directly.
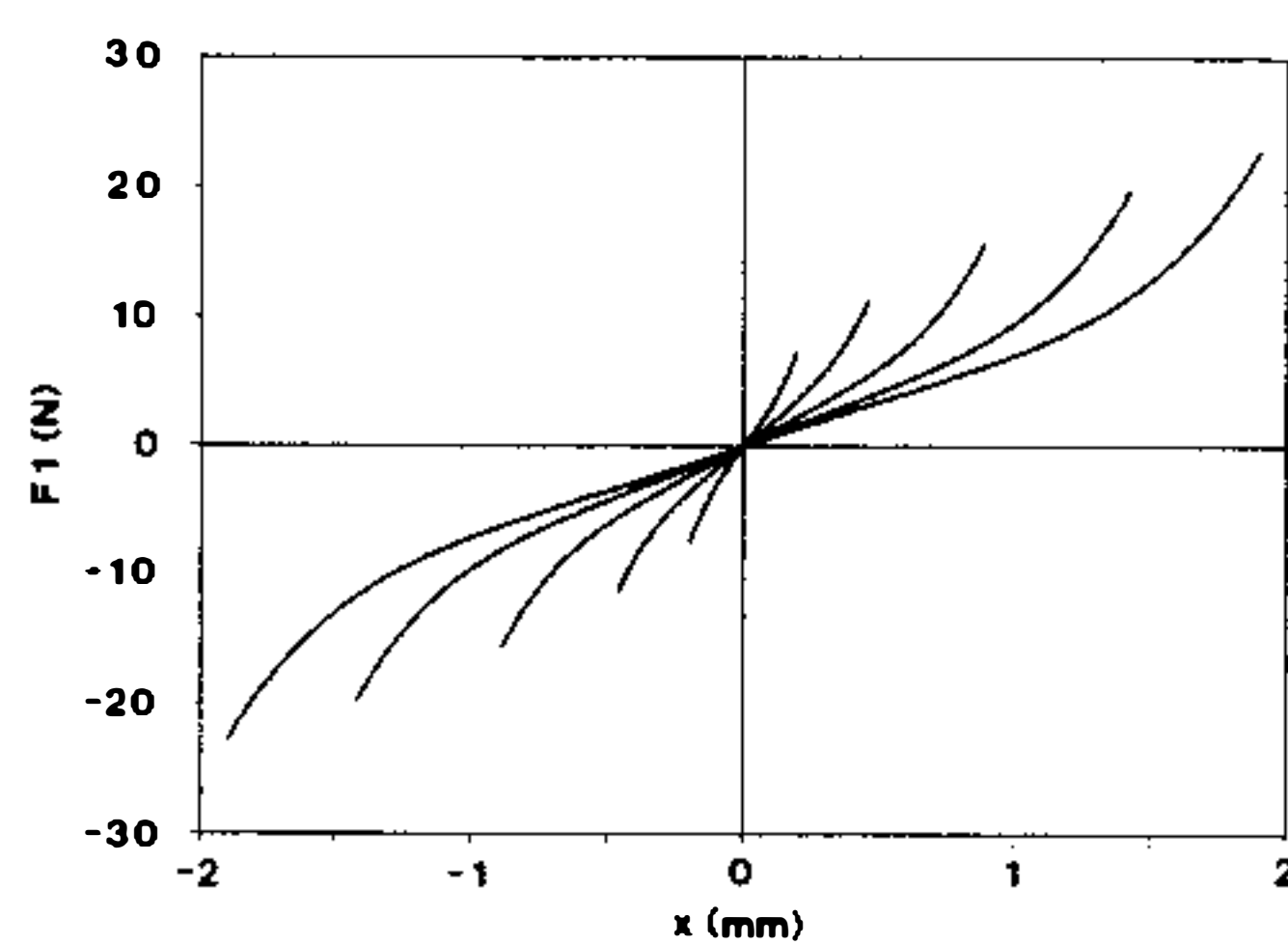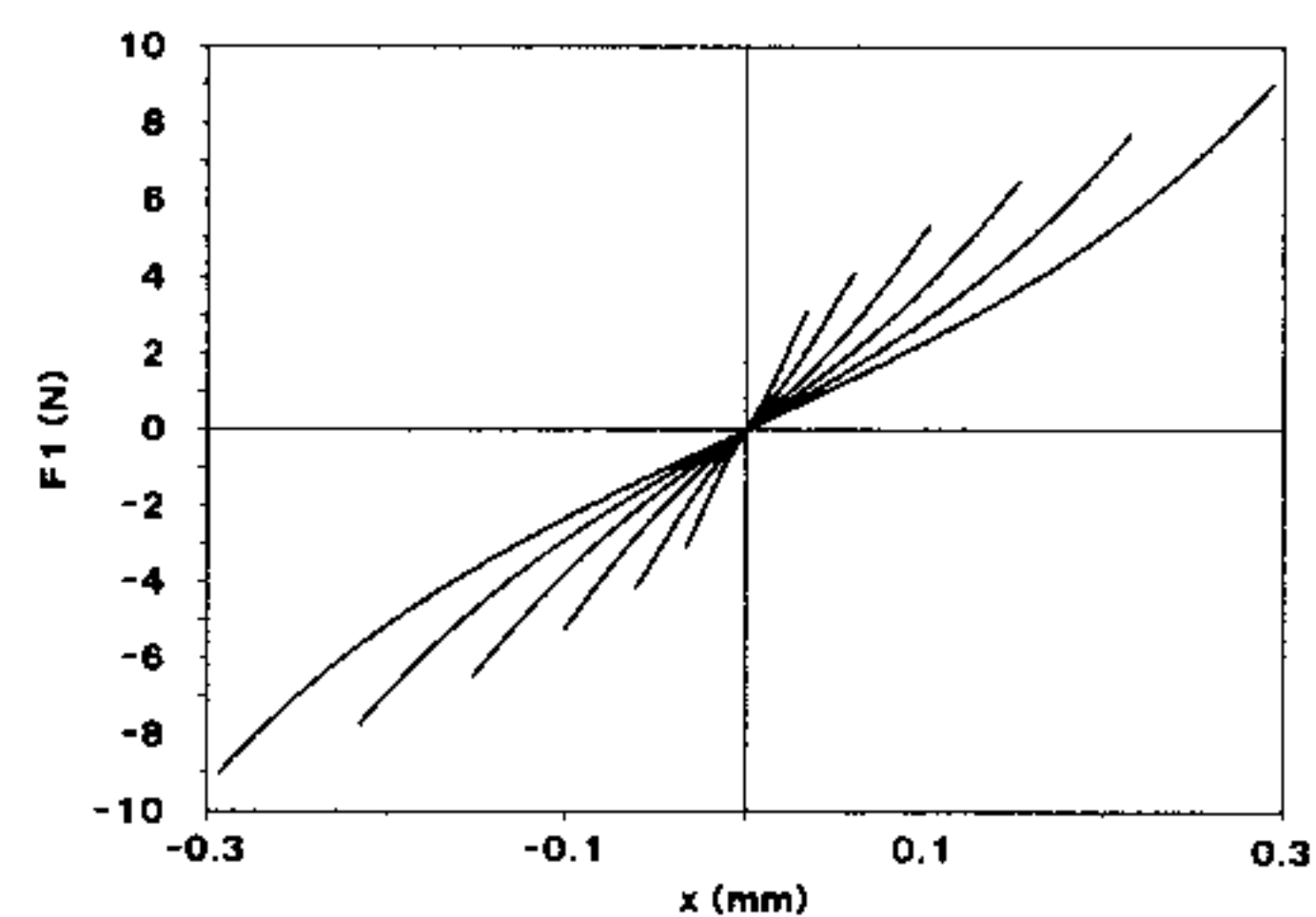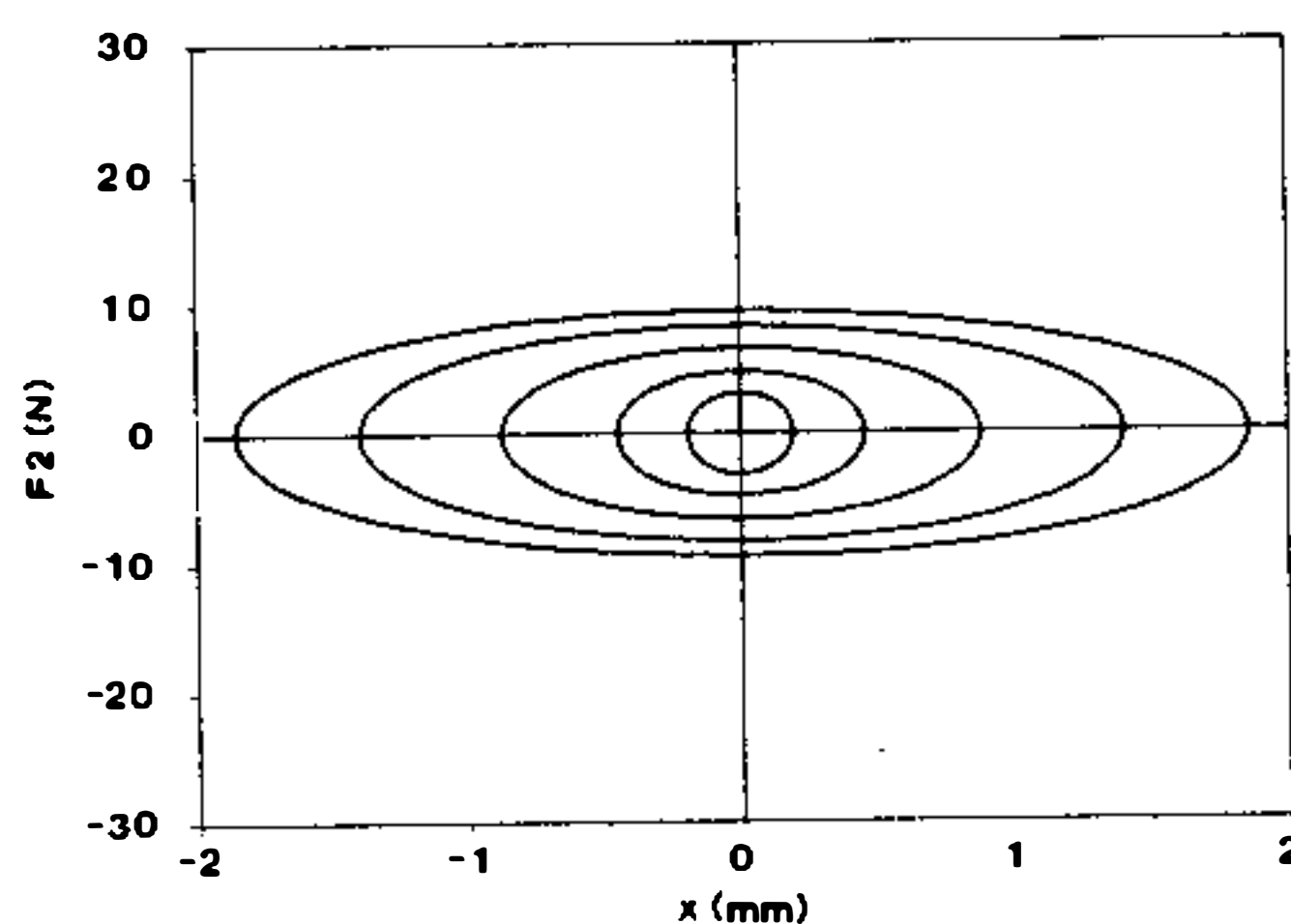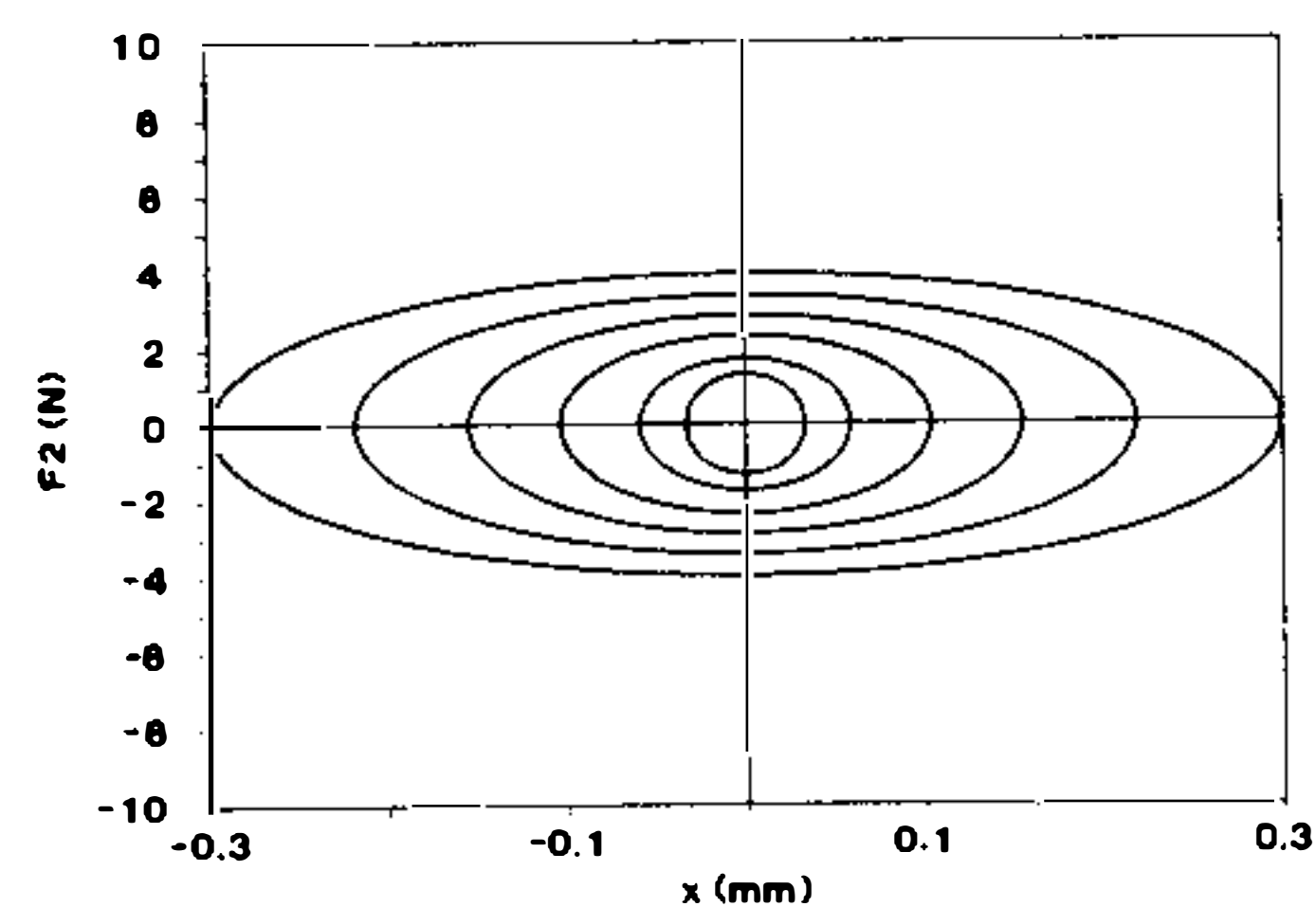

a)   b)

Fig. 14 The function curves of $F_1(x,A)$

a)   b)

Fig. 15 The function curves of $F_2(\dot{x},A)$

When the isolator is in simple harmonic motion, its displacement can be expressed as

$$x(t) = a \cdot \cos \omega t = a \cdot \cos \tau \qquad (29)$$

and the corresponding restoring force is a periodic function, $F(t)$, or written as $F(\tau)$. It can be expanded in a Fourier series

$$F(\tau) = \frac{a^o}{2} + \sum_{i=1}^{\infty} \left(a_i \cos i\tau + b_i \sin i\tau \right) \qquad (30)$$

and

$$a_i = \frac{1}{\pi} \int_{-\pi}^{\pi} F(\tau) \cdot \cos i\tau \, d\tau \qquad (31)$$

$$b_i = \frac{1}{\pi} \int_{-\pi}^{\pi} F(\tau) \cdot \sin i\tau \, d\tau \qquad (32)$$

in which a_i, b_i are the Fourier expansion coefficients of $F(\tau)$ and are known at this stage since they have been previously obtained by the FFT for corresponding restoring force signals.

Remembering that $F(\tau) = F_U(x)\big|_{x=a \cdot \cos \tau}$ for $-\pi \leq \tau \leq 0$ and $F(\tau) = F_L(x)\big|_{x=a \cdot \cos \tau}$ for $0 \leq \tau \leq \pi$ and substituting these and $\tau = \cos^{-1}(x/a)$ into Eq. (31) yield

$$\begin{aligned} a_i &= \frac{1}{\pi} \left[\int_{-a}^{a} F_U(x) \cdot \cos\left\{ i \cos^{-1}(x/a) \right\} \cdot \left\{ +\left(a^2 - x^2\right)^{-1/2} \right\} dx \right. \\ &\quad \left. + \int_{a}^{-a} F_L(x) \cdot \cos\left\{ i \cos^{-1}(x/a) \right\} \cdot \left\{ -\left(a^2 - x^2\right)^{-1/2} \right\} dx \right] \\ &= 2 \int_{-a}^{a} g(x) \cdot T_i(x/a) \cdot r(x) dx \end{aligned} \qquad (33)$$

in which

$$g(x) = \left[F_U(x) + F_L(x) \right] / 2 \qquad (34)$$

$$r(x) = \left[\pi \left(a^2 - x^2\right)^{1/2} \right]^{-1} \qquad (35)$$

and $T_i(x/a) = \cos\{ i \cos^{-1}(x/a) \}$ is the Chebyshev polynomial of the first kind. Similarly Eq. (32) reduces

$$b_i = 2 \int_{-a}^{a} h(x) \cdot D_i(x/a) \cdot r(x) dx \qquad (36)$$

in which

$$h(x) = \left[F_L(x) - F_U(x) \right] / 2 \qquad (37)$$

$$D_i(x/a) = \left[1 - \left(x^2/a^2\right) \right]^{1/2} \cdot U_{i-1}(x/a) \qquad (38)$$

and $U_i(x/a)$ is the Chebyshev polynomial of the second kind.

Let $g(x)$ and $h(x)$ be expanded in the Chebyshev polynomials

$$g(x) = \sum_{i=0}^{\infty} \alpha_i \cdot T_i(x/a) \tag{39}$$

$$h(x) = \sum_{i=0}^{\infty} \beta_i \cdot D_i(x/a) \tag{40}$$

where α_i, β_i are undetermined coefficients. Substituting Eqs. (39) and (40) in Eqs. (33) and (36), and using the orthogonal relationships of Chebyshev polynomials, we obtain

$$\alpha_i = a_i \tag{41}$$

$$\beta_i = b_i \tag{42}$$

Equations (41) and (42) indicate that, if $g(x)$ and $h(x)$ are expanded in Chebyshev polynomials, their coefficients are the Fourier expansion coefficients of restoring force $F(t)$. Thence, according to the known first M order Fourier coefficients, a_i, b_i, of the isolator restoring force, we can directly obtain, in the least mean-squared error sense, the function expressions of hysteresis loops as follows
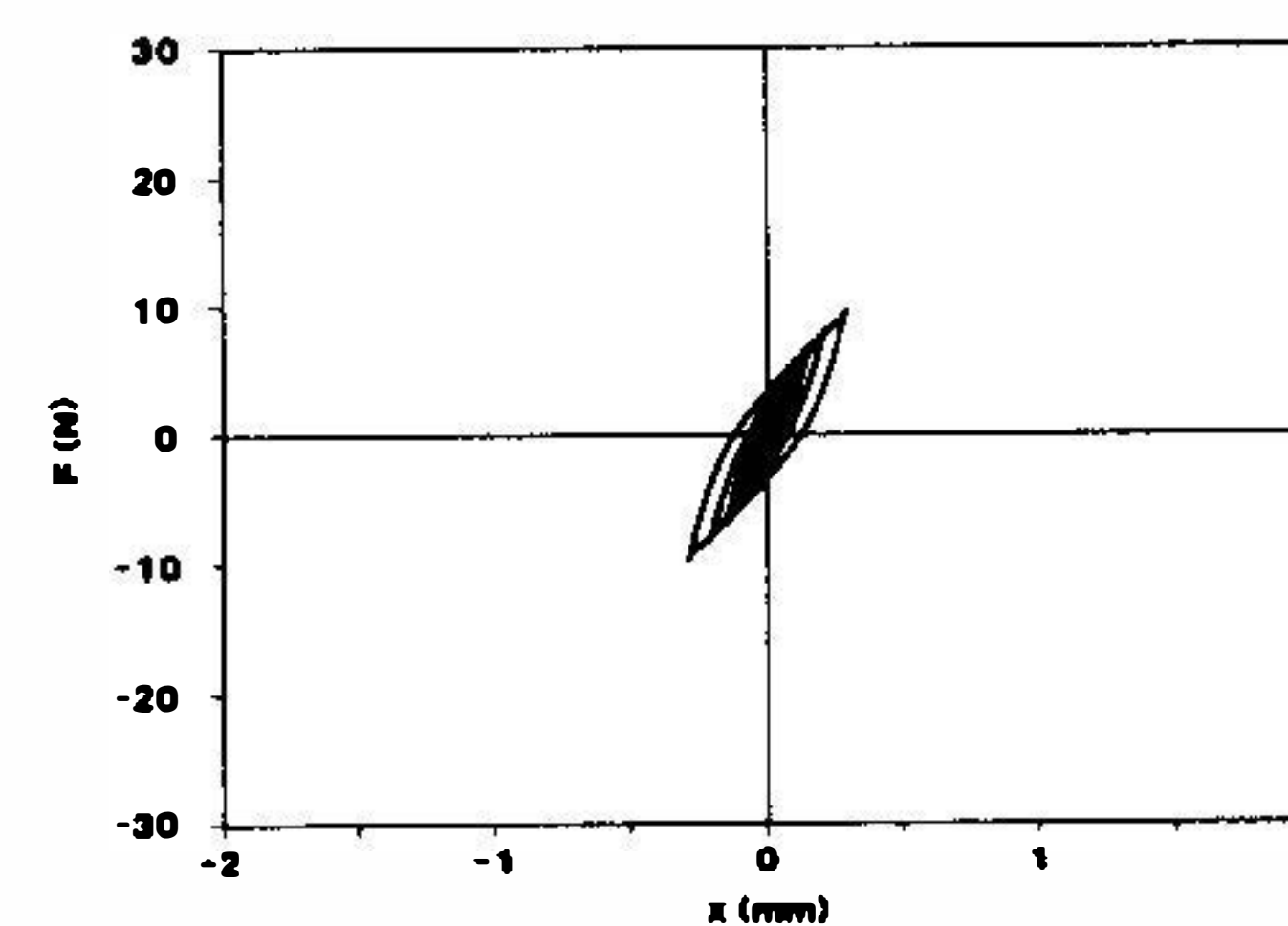
$$g(x) = \sum_{i=0}^{M} a_i \cdot T_i(x/a) \tag{43}$$

$$h(x) = \sum_{i=1}^{M} b_i \cdot D_i(x/a) \tag{44}$$

and

$$F_U(x) = \sum_{i=0}^{M} a_i \cdot T_i(x/a) - \sum_{i=1}^{M} b_i \cdot D_i(x/a) \tag{45}$$
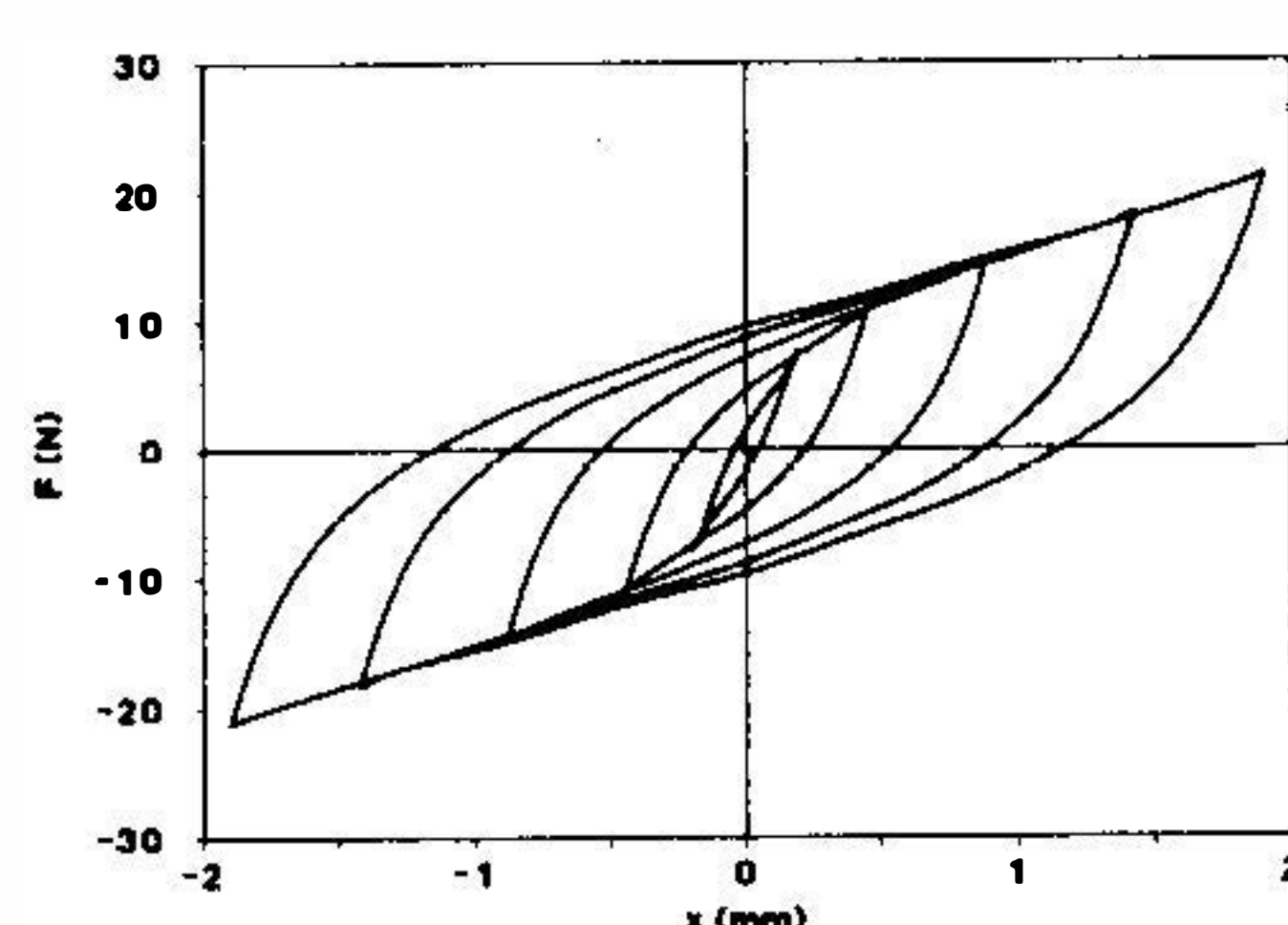
a)   b)

Fig. 16 Direct identification of hysteresis loops

$$F_L(x) = \sum_{i=0}^{M} a_i \cdot T_i(x/a) + \sum_{i=1}^{M} b_i \cdot D_i(x/a)$$
(46)

The above procedure can directly identify the hysteresis loops of the wire-cable isolator. Although the isolator in the experiments was kept, as far as possible, in harmonic motion, it can be seen from Table 1 that the isolator is not always obeying purely simple harmonic motion. However, so long as the higher order harmonic components of the displacement of the isolator are far less important than the first harmonic, as is the case in Table 1, the above procedure can still be applied almost error-free to identify the hysteresis loop functions. In this case, the displacement amplitude A of the isolator should be taken as the value of a in Eqs. (43)-(46) to satisfy the definition of Chebyshev polynomials.

Figures 16(a-b) give the hysteresis loops of the wire-cable isolator at 9 and 20 Hz respectively, obtained by the above procedure. Compared with Figs. 4(b) and 4(c), good agreement can be observed.

5. Concluding Remarks

Dynamic hysteretic behavior experiments of a wire-cable isolator have been carried out. Corresponding experimental data processing and analyzing programs for obtaining hysteresis loops and the mathematical model of restoring force versus displacement have been developed. These experimental and analyzing procedures can be applied to other hysteretic vibration isolators.

A simple mathematical model representing restoring force versus displacement, with amplitude-dependent parameters, has been established based on averaging and equivalence analysis. With this model, the dynamic characteristics of the nonlinear hysteretic isolator can be distinctly represented. The "pure hysteretic" force part, $F_2(\dot{x},A)$, varying with amplitude A, is similar to the damping force of rubber-type viscous isolators. The "nonlinear nonhysteretic" force part, $F_1(x,A)$, is a single-valued function of displacement x but depends on amplitude A. The function curves of F_1-x vary with A. Thence $F_1(x,A)$ is a function of amplitude A. This functionality allows the resonant behavior of hysteretic isolators to be adjusted with different excitation levels, which is the main difference relative to general rubber-type viscous isolators.

An alternative but direct method based on FFT and Chebyshev polynomial approach is presented to identify the hysteresis loop functions of the isolator under steady harmonic motion. Compared with the power polynomial fitting procedure, this method can be used to identify hysteresis loop functions of arbitrary shape, not only symmetric. Therefore this method is specially useful for cases with different physical conditions under loading and unloading and with preloaded or predeformed isolators. Since this method is based on the assumption that the isolator is under simple harmonic motion, the identification precision depends on the degree to which the condition above is satisfied.

Acknowledgments

References

1. LeKuch, H. "Shock and vibration isolation in severe environments." *Noise Vib Control World wide* v 17 n 8 p 240-245 Sept. 1986.

2. Cutchins, M. A.; Cochran, J. E. ; Guest, S.; Fitz-Coy, N. G.; Tinker, M. L. "An investigation of the damping phenomena in wire rope isolators." In: Rogers, L.; Simonis, J. C. (editors). *The Role of Damping in Vibration and Noise Control.* New York: ASME; 1987. p 197-204

3. Lo, H. R.; Hammond, J. K.; Sainsbury, M. G. "Nonlinear system identification and modelling with application to an isolator with hysteresis." *Proceedings of the 6th International Modal Analysis Conference,* Kissimmee, FL, Feb 1-4, 1988. v 2 p 1453-1459

4. Hu, H. Y.; Li, Y. F. "Parametric identification of nonlinear vibration isolators with memory." *J Vib Eng* v 2 n 2 p 17-27 1989. (In Chinese)

5. Worden, K. "Data processing and experiment design for the restoring force surface method, Part I: Integration and differentiation of measured time data." *Mech Syst Signal Process* v 4 n 4 p 295-319 1990.

6. Bouc, R. "Forced vibration of mechanical system with hysteresis." Abstract, *Proceedings of the 4th Conference on Nonlinear Oscillation,* Prague, Czechoslovakia, 1967. p 315

7. Wen, Y. K. "Method for random vibration of hysteretic systems." *ASCE J Eng Mech Div* v 102 n 2 p 249-263 Apr 1976.

8. Wen, Y. K. "Equivalent linearization for hysteretic systems under random excitation." *J Appl Mech* v 47 p 150-154 1980.

9. Baber, T. T.; Noori, M. N. "Modelling general hysteresis behavior and random vibration application." *J Vib Acoust Stress Reliab Des* v 108 p 411-420 1986.

10. Roberts, J. B.; Spanos, P. D. *Random Vibration and Statistical Linearization.* New York: John Wiley & Sons; 1990.

11. Badrakhan, F. "Rational study of hysteretic systems under stationary random excitation," *Int J Non Linear Mech* v 22 n 4 p 315-325 1987.

12. Badrakhan, F. "Dynamic analysis of yielding and hysteretic systems by polynomial approximation." *J Sound Vib* v 125 n 1 p 23-42 1988.

13. Wong, C. W.; Ni, Y. Q.; Ko, J. M. "Steady state dynamic response analysis of vibration-isolated structure with nonlinear hysteretic isolators." Submitted to *Int J Anal Exp Modal Anal*

14. Atherton, D. P. *Nonlinear Control Engineering.* London: Van Nostrand Reinhold; 1982.

VII International Congress on EXPERIMENTAL MECHANICS and Manufacturers Exhibit

Riviera Hotel
Las Vegas, Nevada, U.S.A.

June 8-11, 1992

Co-Sponsored by: Society for Experimental Mechanics, Inc., American Society for Nondestructive Testing, British Society for Strain Measurement, European Permanent Committee for Experimental Mechanics, IMEKO-TC 3 and TC 15, Italian Association for Strain Analysis, Japan Society of Mechanical Engineers, Korean Society of Mechanical Engineers, SEM Republic of China Section - Taiwan, Shock & Vibration Information Analysis Center, Slovene Society for Experimental Mechanics, Strain Society for South Africa, VDI/VDE Gesa

For additional information contact: Kathy Ramsay, SEM Conference Manager or Kathy Richter, SEM Exhibits Manager, Society for Experimental Mechanics, Inc., 7 School Street, Bethel, CT 06801, U.S.A.

17th International Seminar on MODAL ANALYSIS AND STRUCTURAL DYNAMICS

Leuven, Belgium

September 21-25, 1992

For additional information contact: Prof. P. Sas, Katholieke Universiteit Leuven, Division PMA (Production Engineering, Machine Design and Automation), Celestijnenlaan 300B, 3001 Leuven, Belgium. Tel: (32) 16 28.66.11 2480, Telex: 23674 kuleuv b, Fax: (32) 16 22.23.45